Institute of Polar Studies
Report No. 16

An Examination and Analysis of the Formation of Transverse Crevasses, Kaskawulsh Glacier, Yukon Territory, Canada

by

Gerald Holdsworth
Institute of Polar Studies

August 1965

The Ohio State University
Columbus, Ohio 43210

Director

INSTITUTE OF POLAR STUDIES

Report No. 16

AN EXAMINATION AND ANALYSIS OF THE FORMATION OF TRANSVERSE CREVASSES, KASKAWULSH GLACIER, YUKON TERRITORY, CANADA

by

Gerald Holdsworth

Institute of Polar Studies

June 1965

The Ohio State University
Columbus, Ohio 43210

ABSTRACT

The main purpose of this investigation was:
(1) to examine the applicability of Nye's theoretical expression for the longitudinal strain rate on the surface of a valley glacier; namely to test whether:

$$\dot{\epsilon}_x = mV_b (mV_b + u_s)^{-1} \left(\frac{a}{h} + u_s \pi \cot\alpha - \frac{1}{h}\frac{\partial h}{\partial t} - \dot{e}_y + \frac{1}{2} h \nabla \frac{d\pi}{dx} \right)$$

and (2) to investigate the mechanics and mode of formation of transverse crevasses.

In an area at the head of a valley glacier a regional strain rate field was derived from velocity and strain net measurements. The result of a comparison between measured and computed strain rates is inconclusive because the assumptions on which the theoretical equation is dependent are not valid except in one short section, where an approximate agreement is found.

A value of regional longitudinal extending strain rate of about 3.5×10^{-5} day^{-1} is associated with the occurrance of the first transverse crevasse in previously unfractured firn. The strain rate gradient and hence the rate of stress development associated with this critical strain rate is considered to be important. Localized strain rates and stresses of at least an order of magnitude greater than regional values are deduced to be responsible for fracturing of ice.

Regional values of strain rate do not give a theoretical depth of crevasses close to the observed values. Strain rates of at least an order of magnitude greater are required to produce a rough agreement.

Crevasse spacings average 2.8 x mean crevasse depth, which is about 26 meters. Some methods of computing crevasse spacings are given. Nielsen's formula gives a spacing close to the mean of the measured spacings.

A concept of the formation of transverse crevasses is discussed. This follows closely the hypothesis of Meier. The crevasses appear to be forming at the margins of the ice stream and to be propagating quietly towards the center; a plastic rather than an elastic behavior is thus suggested. Suitably placed seismograph stations could be used to locate initial points of failure within the ice.

CONTENTS

	page
List of Figures	v
List of Plates	vii
List of Tables	vii
List of Symbols Used in Text	viii
Introduction	1
Statement of Problem	1
Implications of Research Problem	1
Geography of the Kaskawulsh Glacier Area	3
General Geology in the Area of Crevasse Camp	4
Theoretical Considerations	6
The Rheology of Ice	6
Review of the properties and behavior of ice	6
The fracture of ice	7
Definition of "crevasse"	9
Stress Conditions Existing in Flowing Ice	10
Stress distribution with depth	10
The depth of crevasses	10
Extending and compressive flow	12
Surface stress distribution	14
Consideration of Longitudinal Strain Rate	16
Crevasse Spacing	20
Field Methods	24
General Introduction	24
Velocity Distribution Survey	25
Strain Net Survey	25
Gravity Survey	26
Crevasse Survey	26
Field Data Reduction and Results	27
Velocity Determination	27
Regional Strain Rate Computations	28
Estimate of critical strain rate	31
Gravity Survey Computations	32
Miscellaneous Computations	34
Accumulation and Ablation Data	35
Accumulation	35
Ablation	36
Use of data	37

CONTENTS (cont.)

	page
Field Measurements of Crevasse Depths	37
General data	37
Kaskawulsh glacier transverse crevasse depths	39
Field observations of crevasse spacing	39
Calculation of crevasse spacing	43
Calculation of theoretical longitudinal surface strain rate	44
Discussion of Data and Results	47
Discussion of Velocity Data	47
Discussion of Strain Rate Data	48
Accumulation effect	48
Curvature effect	49
Transverse strain rate	50
Rate of ice thickness change	50
Bending effect	50
Comparison of Measured and Theoretical Values of Longitudinal Strain Rate	50
Discussion of Previous Comparisons Between Measured and Computed Strain Rates	51
Comparison of Laboratory and Field Measurements of Strain Rates	52
Discussion of Crevasse Depths	53
Discussion of Crevasse Spacing	56
General Concept of Transverse Crevasse Formation	58
Acknowledgements	60
References	62
Appendix I. Notes on the Morphology and Stratigraphy of Crevasses	66
Appendix II. Meteorological Data	69
Appendix III. Computation of Surface Stresses	71
Appendix IV. Comparison of Theoretical Crevasse Depths Using Two Flow Laws for Ice	73

Figures

		Page
1.	Locality map. Crevasse Camp (2435 m.) is at latitude 61°46'N., longitude 139°30'W. Divide Camp (2640 m.) is at latitude 61°46'N., longitude 139°40'W.	74
2.	Geometry of the survey network and the configuration of the transverse crevasse field.	75
3.	Computed cross-sections of Kaskawulsh Glacier between stations H and K.	76
4.	Generalized relations between (A) applied stress and strain rate: 1, Newtonian liquid; 2, perfectly plastic solid. K is the yield stress; 3, ice (after Glen, 1952); and (B) ultimate tensile strength and rate of loading of ice (after Butkovich, 1958).	76
5.	(A) Stress block for element of ice subjected to extending flow. (B) Mohr's circle construction for finding principal stresses. (C) Principal axes of stress. (D) Typical crevasse patterns. Transverse fractures are associated with $\sigma_1 > 0 > \sigma_2$. Longitudinal fractures are associated with $\sigma_2 > 0, \tau_{xy} \leq \left\lvert \frac{\sigma_2}{\sqrt{2}} \right\rvert$. Ice flows to right. (E) Limiting case where $\sigma_2 \geq 0$.	77
6.	Plot of crevasse spacing with distance down glacier.	77
7.	Configuration of flow-line field based on velocity data.	78
8.	Contours of total velocity V, m. day^{-1}.	79
9.	Contours of velocity component V_X, m. day^{-1}.	79
10.	Contours of velocity component V_Y, m. day^{-1}.	79
11.	Contours of principal extending strain rate ($\dot{\epsilon}_1$).	80
12.	Contours of principal contracting (least extending) strain rate ($\dot{\epsilon}_2$).	80
13.	Contours of maximum shearing strain rate ($\lvert \dot{\epsilon}_1 - \dot{\epsilon}_2 \rvert$).	80
14.	(A) Configuration of principal strain rate field in region of the transverse crevasses. (B) Longitudinal variation of principal extending strain rate.	81

15. (A) Approximate extending strain rate gradient perpendicular to crevasse traces ($\frac{\dot{W}_c}{S}$). (B) Variation of crevasse opening rate ($\dot{W}_c$) down glacier. (C) Surface width (W_c) and spacing (S) of crevasses 3 to 9. 82

16. Longitudinal profile of glacier surface and bedrock along central markers 1 through 4 (located in Figure 2). Sources of data are given. 83

17. Average surface configuration, July 1964. Flow-line through marker 4 is the "dynamic" center-line; flow-line through 1 and 2 is the "geographic" center-line. 84

18. Stratigraphic, geophysical and morphological features of a typical crevasse. 85

19. Sections across crevasses no. 10 and no. 14 in the region of the snow-bridge. 86

Plates

		Page
1.	View S.W. from Divide Camp showing barrier of Mt. Logan Massif. Foreground topography is typical of the divide and upper North Arm of the Kaskawulsh Glacier.	87
2.	View N.E. from Crevasse Camp looking down the North Arm of the Kaskawulsh Glacier.	87
3.	Aerial view of Crevasse Camp and transverse crevasse field. Line of pits is perpendicular to the crevasse traces which are convex up glacier.	88
4.	Aerial oblique view of the crevasse field. Crevasse Camp is just visible.	88
5.	Aerial oblique view showing the geometry of the transverse crevasses. To the south a small ice-fall and marginal crevasses complicate the regional pattern.	89
6.	View looking upward through the snow-bridge, from 20 meters below the surface.	89
7.	Icicles on base of snow-bridge.	90
8.	Crevasse wall growths and icicles.	90

Tables

1.	Accumulation on the North Arm of Kaskawulsh Glacier.	36
2.	Crevasse Depths.	40
3.	Computation of $\bar{\nabla}\pi c \cot\alpha$ From Surface Data.	45
4.	Computation of $\bar{\nabla}\pi c \cot\beta$ From Bed Profile Data.	45
5.	(a) List of Component Strain Rates	46
	(b) Comparison Between Computed and Measured Strain Rates.	
6.	Comparison of $\dot{\epsilon}_{xx}$(Calculated) and $\dot{\epsilon}_{xx}$(Measured) For Athabaska Glacier, Canada (after Paterson, 1962).	52

List of Symbols Used in Text

		Dimensions
a	accumulation term (expressed as ice equivalent), negative if ablation.	$L.\ T^{-1}$
A	area of cross-section	L^2
B, B′	empirical constants	
d	depth of crevasses	L
g	acceleration of gravity	$L.\ T^{-2}$
G_ϕ	gravity value on the international reference ellipsoid at latitude ϕ	$L.\ T^{-2}$
h	ice thickness at any position	L
K	yield stress of ice on perfect plasticity theory	$M.\ L^{-1}.\ T^{-2}$
l_i	length	L
m	empirical constant $\frac{n+1}{2} \simeq 2.1$ (temperate ice)	
n	empirical constant in flow law. ~3.17 for temperate ice	
p	perimeter of ice in contact with bedrock measured in a cross-section perpendicular to the glacier surface	L
P	constant (air pressure)	$M.\ L^{-1}.\ T^{-2}$
q	rate of flow of ice per unit width at the centerline of flow	$L^2.\ T^{-1}$
Q	total rate of ice flow through a given cross-section	$L^3.\ T^{-1}$
R	radius of curvature of a given surface	L

s	crevasse spacing	L
S	ultimate bending strength of ice	M. L^{-1}. T^{-2}
t	time	T
u_s	velocity component parallel to the glacier surface	L. T^{-1}
v_s	velocity component perpendicular to the glacier surface	L. T^{-1}
V	total velocity at a given point	L. T^{-1}
V_X, V_Y	velocity components in direction of X, Y axes	L. T^{-1}
$\overline{V}$	mean velocity of ice flowing through a given cross-section	L. T^{-1}
V_b	velocity of ice at the base of the glacier	L. T^{-1}
V_c	surface velocity on central flow-line	L. T^{-1}
$\overline{V}_c$	mean surface velocity, over the depth	L. T^{-1}
$\overline{V}_s$	mean surface velocity, over the width	L. T^{-1}
W	glacier width	L
w_c	crevasse width	L
x', y', z'	rectangular coordinate axes established for each strain diamond	
x, y, z	rectangular curvilinear coordinate axes, where x is in the direction of ice flow, y is transverse and z is perpendicular to x and y	
X, Y	rectangular axes established by Wood in 1961 (see Figure 2)	
α	surface slope measured from the horizontal in the direction of a flow line	
β	bed slope measured in the same manner as α	

$\dot{\gamma}_{xy}$	shearing strain rate in the direction of the y axis and on a plane perpendicular to the x axis	T^{-1}
$\dot{\epsilon}_{x,y,z}$	strain rates in the direction of the x,y,z axes respectively	T^{-1}
$\dot{\epsilon}_1$	maximum (most extending) principal strain rate	T^{-1}
$\dot{\epsilon}_2$	minimum (least extending) principal strain rate	T^{-1}
$\dot{\epsilon}_\varphi$	"unweighted" strain rates referred to direction at center of each strain diamond; $\varphi = 0^o$ along the down glacier diagonal	T^{-1}
$\dot{\epsilon}_c$	critical extending strain rate for fracture of glacier ice	T^{-1}
$\dot{e}$	effective strain rate	T^{-1}
θ	angle between the x axis and the axis of principal extending strain rate; measured in the x,y plane	
ρ	density of glacier ice (0.9 gm. cm^{-3})	$M. L^{-3}$
σ	effective "hydrostatic" stress	$M. L^{-1}. T^{-2}$
$\sigma_{x,y,z}$	normal stresses in direction of x,y,z axes	$M. L^{-1}. T^{-2}$
σ_c	critical tensile stress associated with rupture	$M. L^{-1}. T^{-2}$
$\sigma_{1,2,3}$	principal stresses at a point	$M. L^{-1}. T^{-2}$
$\sigma'_{1,2,3}$	principal stress deviators at a point	$M. L^{-1}. T^{-2}$
τ	effective shear stress	$M. L^{-1}. T^{-2}$
τ_b	basal shear stress	$M. L^{-1}. T^{-2}$
τ_{xy}	shear stress in direction y, on a plane perpendicular to the x axis	$M. L^{-1}. T^{-2}$
κ	curvature, ($=R^{-1}=\frac{d\alpha}{dx}$)	L^{-1}
$\cdot$	denotes differentiation with respect to time	T^{-1}

INTRODUCTION

Statement of Problem

In recent years the theory of glacier mechanics has received much attention, especially from J. F. Nye and J. Weertman. As a result of the steady accumulation of physical theory, associated with certain controversial problems, it has become necessary to test the mathematical deductions by conducting precise observations on accessible glaciers. M. F. Meier, J. F. Nye, W. S. B. Paterson and many others have made significant contributions in this field.

The greater part of this thesis represents an attempt to verify a theoretical relation, derived by Nye (1951, 1959a, 1959b, 1959c) which relates the longitudinal rate of strain in a glacier to physical characteristics of the ice mass. An attempt is also made to relate the strain rate field to the occurrence of transverse crevasses. Certain aspects of the geometry of these crevasses are investigated.

Implications of Research Problem

Previous work that has included an attempt to test the theoretical relation for the longitudinal surface strain rate in a glacier (Paterson, 1962) shows inconclusive results. Thus it is considered that a more exhaustive investigation is warranted.

The rheological aspects of the study are at once apparent. Attention is drawn to the behavior of the flow, deformation and fracture of a sedimentary-diagenetic crystalline aggregate close to or at its pressure melting point.

Structural geologists and glaciologists are faced with many analogous problems. Much of the information obtained from the observations of the dynamics and fracture of glacier ice can be applied to problems involving "hot creep" deformation and fracture of subcrustal rock material which is at present inaccessible to direct observation. Such concepts have been considered in theses on continental drift (e.g. Orowan, 1964). Rock joints, which are produced by anisotropic stress conditions of mechanical or thermal origin, are closely analogous to crevasses in glacier ice, but certain significant differences exist so that the stress analyses may not be similar in the two cases.

Some important ideas relating to the flow and fracture of crystalline materials have arisen from metallurgical research. Investigations have been made on the deformation and fracture mechanisms of polycrystalline magnesium at low temperatures (Hauser, Landon and Dorn, 1956). In recent years the analogies between the rheology of ice and of certain metals has become evident and much of the work in the two fields is clearly complementary. It is worth noting that because many glaciers are at, or near the melting point, the rheological processes are more rapid here than at low temperature (Glen, 1955), whereas most metals generally require considerably elevated temperatures for comparable rates of deformation.

Practical applications of crevasse mechanics also exist. When planning overland traverses, polar and alpine research expeditions are frequently faced with logistical problems which are created when routes traverse regions of crevassed ice. Consequently, a detailed knowledge

of the geometry of certain basic crevasse types is essential. Schuster (1954) discusses travel and rescue in crevassed areas.

Geography of the Kaskawulsh Glacier Area

A portion of the Icefield Ranges, lying within the St. Elias Mountains, Yukon Territory, Canada is shown in Figure 1. From the extensive névé field in the region of latitude 61° 45' N., longitude 139° 30' W., ice flows south-westward as the Hubbard Glacier, and eastward towards inland Yukon, as the Kaskawulsh Glacier. According to the terminology of Hobbs (1911) the whole system may be classified as a linearly opposed transection glacier with a broad common snow and ice divide. This firn field reaches a maximum altitude of 2640 meters above sea level, while most of it lies above 2500 meters. The greater part of the ice is over 500 meters thick (Clarke, pers. comm.). Rock and ice peaks on the northern and southern edge of the catchment area rise to 3500 meters above sea level. Farther to the south and west massive mountains of which the most prominent is Mount Logan (5900 m.) (Plate 1.), form a topographic barrier sufficient to influence the meteorological regime of this highland area. There exists, for instance, a significant gradient in the net mean annual accumulation of snow. At the divide area an average of 180 $gm.cm.^{-2}yr.^{-1}$ accumulates whereas in the upper Kaskawulsh Glacier 110 to 120 $gm.cm.^{-2}yr.^{-1}$ accumulates. Furthermore, summer meteorological records show a remarkably low mean wind velocity. This has a pronounced effect on the micro-relief of the glacier surfaces and to a certain extent on the process of bridging of crevasses (Appendices I and II).

During the summer of 1961, Ragle (in Wood, 1963) measured a temperature profile in the firn near Divide Camp (Figure 1). Here he determined that a uniform temperature of -0.5^{o} C existed to 15.5 meters depth, and he subsequently classified the ice in the region of the divide as subpolar in character (Ahlmann, 1948). Observations of snow stratigraphy apparently supported this conclusion. During the summer of 1964, Higashi and Shimizu (pers. comm.) working in the same locality determined that the 0^{o} C isotherm existed to 15 meters depth. Measurements of temperature within several crevasses 15 kilometers to the east of the divide suggests that the ice in this area is temperate. A fuller discussion of these observations is given in Appendix I.

Wagner (1963, 1964) recognized that the area near the head of the Kaskawulsh Glacier lies within the saturation zone. This area also lies well above the firn limit which is at 2150 meters. The first transverse crevasse field coincides approximately with the formation of the North Arm of Kaskawulsh Glacier at 2450 meters (Figure 2).

The present project area included four square kilometers of glacier surface located at approximately latitude 61^{o} 47' N. and longitude 139^{o} 28' W. and covering part of the upper North Arm of Kaskawulsh Glacier. Observations were conducted here for seven weeks between July 4 and August 15, 1964.

General Geology in the Area of Crevasse Camp

Existing geological maps do not provide information in the area west of the junction of the North and Central Arms of the Kaskawulsh Glacier (Wheeler, 1963). About 16 km. west of the limits of these maps

and in the area of Crevasse Camp (Figure 2 and Plates 2, 3, 4, and 5) three main outcrops were accessible. Paleozoic (Devonian?) fossiliferous limestones and dolomites crop out on peaks on the north side of the glacier. The southern side of the glacier is flanked by nunataks of hornblende granodiorite probably of Cretaceous age. No contact with the sedimentary rocks was observed. Intruding the granodiorite, however, are a number of basic (dolerite) dikes of Lower Tertiary (?) age. Intrusives of a more acidic nature (trachytes to rhyolites) occur in much of the limestones. Morainal material was absent on these outcrops.

It is necessary to consider the nature and distribution of the rock assemblages present in order to estimate a value of average bedrock density which is used in reducing gravity data, from which an estimate of ice thickness can be made. In this area the rock densities are estimated to vary from about 2.6 to 2.8 gm.cm.$^{-3}$ (Dobrin, 1960, p. 251). It was expected that an asymmetrical bedrock profile might have been developed due to differential erosion, because the granite-sedimentary contact is somewhere beneath the ice. The cross-section given in Figure 3, however, does not show this.

"The glacier suddenly cracks open with a loud report, the surface shakes, and a long narrow crack appears in the ice. A crack about half an inch wide and several hundred feet long appears to be a typical baby crevasse."

-L. E. Nielsen in the American Alpine Journal (1958).

THEORETICAL CONSIDERATIONS

The Rheology of Ice

Review of the properties and behavior of ice

Early analyses (e g. Lagally, 1929) of the flow and fracture behavior of ice were based on the assumption that ice exhibited the properties of a Newtonian fluid. As new data became available, it was found necessary to revise certain assumptions regarding the properties of ice. Recent works (e.g. Nye, 1951 to 1963) which develop the theory of glacier flow, have initially assumed, to simplify calculations that ice behaves as a perfectly plastic solid. That this is a substantial simplification is well known. Figure 4-A shows the relationships between applied stress and strain rate in a material of constant viscosity (1) and in a perfectly plastic material (2) in which the yield stress is K. Curve (3) shows the observed general relationship for ice.

Glen (1952, 1953, 1955), Butkovich and Landauer (1959), and others have shown that a flow law exists of the general form, $\dot{\epsilon} = B\sigma^n$ (for $\sigma \geq$ 0.6 bars) for the material ice when subjected to shear, compressive or tensile stresses. Rigsby (1958) has shown that for single ice crystals the flow law is independent of hydrostatic pressure and this also appears to be valid for polycrystalline ice. This condition holds provided that the difference between the ice temperature and the pressure melting

point is kept constant. Crystallographically, ice belongs to the hexagonal system and experiments by Steinemann (1958) and others show that to a good approximation "glide" occurs only along the basal plane (0001). From the flow law and from general observations it is apparent that ice can exhibit the properties of either a "visco-plastic", a plastic, or a "plasto-elastic" material depending on the magnitude and development of the applied stress. To develop these ideas further it is necessary to refer to the work of Butkovich (1958, p. 2), who examined the behavior of standard cylinders of ice under tensile stresses at different rates of loading. The average tensile strength is related to the rate of stress application within the ice (Figure 4-B). A "visco-plastic" response occurs below a loading rate of approximately 0.5 kg.cm.$^{-2}$ sec.$^{-1}$, whereas above this value, a "plasto-elastic" type of response is observed in which the ultimate tensile strength is essentially independent of loading rate. These observations are pertinent in considering the nature of rupture of glacier ice.

The fracture of ice

In the analyses which follow, ice will be regarded as homogeneous and isotropic. This is a substantial simplification. Furthermore, it will be assumed that the crystallographic orientation of the ice is random. Under these conditions, Glen (1963) has assumed that the maximum principal stress parallels the direction of maximum strain rate in the general case. For other than randomly orientated ice the magnitude of the stress determines the direction of maximum strain. Finally, the effect of temperature on the rheological behavior of ice must be recognized.

Glen (1963) states that a reduction in temperature from 0^{o} C to -15^{o} C reduces the flow rate by an order of magnitude. He has shown specifically that the value of B in the flow law is an exponential function of temperature. The fact that the value of B is extremely sensitive to changes in temperature is discussed in a later chapter.

Ice will fracture under tensile or compressive loading (Gold, 1960), but this analysis will consider only tensile failure of glacier ice. For tension failure to occur, the applied stress within the ice must exceed the ultimate tensile strength. In true glacier ice, the u.t.s. will depend on the direction of stress application, the magnitude of the other principal stresses, the ice temperature, and the bulk physical properties of the ice of firn. Average tensile strengths of ice are given in S.I.P.R.E. Report 4 (1951) but the nature of the laboratory tests and the complete physical condition of the ice are not fully specified. Values of u.t.s. ranging from 2.5 kg.cm.$^{-2}$ to 18.0 kg.cm.$^{-2}$ have been found. Other sources give values ranging from 6.5 to 17.0 kg.cm.$^{-2}$. However, there seems to be little correspondence between laboratory and field measurements of the tensile strength of ice. Calculations by Nye (1959b) indicate that glacier ice will fracture when subjected to tensile stresses of the order of two bars, but others (e.g. Lliboutry, 1958) have maintained that higher stresses, of the order of 5 to 12 bars, are necessary. It should be understood, however, that the upper parts of most glaciers are not "pure" ice. Furthermore, as will be elaborated later, there is reason to believe that the regional stresses on the surface of a glacier are not necessarily indicative of local stresses which have a greater significance in terms of

failure mechanics. Because the surface strain rate only is measured, it is convenient to relate failure of the ice in tension to a critical surface strain rate, but the gradient of strain rate at any point must be specified. In other words, the rate of loading or stress application is important. The stresses are generally considered to be mechanically produced, but there is some evidence to suppose that stresses of thermal origin may be significant (Mellor, 1964). It has been estimated that stresses sufficient to break ice can be produced by a temperature change of about 20^{o} C in the upper five meters of a glacier, but the time of temperature change is not given (Bull, pers. comm.).

Nielsen (pers. comm.) and others have witnessed the formation of a transverse crack and describe the phenomenon as being associated with an audible energy release and detectable surface waves. Such a description suggests that ice can exhibit an "elasto-plastic" behavior.

Definition of "crevasse"

The origin of the term crevasse is not discussed here, but it was evidently in use in the literature of the eighteenth century alpinists. Meier (1960, p. 57) distinguishes between crevasses and cracks by assigning an arbitrary upper limit of 30 centimeters width to define cracks. Since there is no mechanical or genetic significance implied in this definition, it will not be used here. Instead, the term "crack" will be used to imply an ice or firn fracture which possesses no measurable opening. Thus, cracks are incipient crevasses. All fractures possessing a measureable opening that occur in the surface zones of a glacier are regarded as crevasses. A particular class, namely transverse crevasses, will be

considered here. Although marginal crevasses do occur in the area the mechanics of these are not discussed.

Stress Conditions Existing in Flowing Ice

Stress distribution with depth

Prandtl (1923) has provided the stress solution applicable to a system in which a perfectly plastic material is compressed in plane strain between two parallel plates spaced 2h apart. The plates are inclined at an angle α to the horizontal and that part of the system below z = h is considered as a model glacier. Reference axes are taken at the bed on which $\tau_{xz} = K$, the yield stress.

Nye (1951, p. 557, 1957c) gives the following solution:

$$\sigma_x = x\left(\frac{K}{h} - \rho g \sin\alpha\right) + z\rho g\cos\alpha \pm 2K\sqrt{1-\left(1-\frac{z}{h}\right)^2} + P \qquad (1)$$

$$\sigma_z = x\left(\frac{K}{h} - \rho g \sin\alpha\right) + z\rho g\cos\alpha + P \qquad (2)$$

$$\tau_{xz} = K\left(1 - \frac{z}{h}\right) \qquad (3)$$

for a material of density ρ .

The depth of crevasses

It is required to find the depth z to which σ_x is still tensile. By placing $\sigma_x = 0$, in equation (1) and using (2),

$$\sigma_z = 2\sqrt{K^2 - \tau_{xz}^2}$$

and substituting for σ_z and τ_{xz} ,

$$z = \frac{2K}{\rho g\sqrt{1 + 3\sin^2\alpha}}$$

If α is small,

$$z \simeq \frac{2K}{\rho g} \qquad (4)$$

Taking K as one bar, $z \simeq 23$ meters. This, then, is the depth to which a crevasse might open. Alternatively, it is possible to consider a fracture that has already formed and opened to a depth which is greater than 23 meters, but that the extending strain rate is then released. If the normal stress due to air pressure is P, then at a certain depth the lateral stress on the crevass wall is 2K + P, where 2K is the yield stress in compression. This is equated to an equivalent hydrostatic stress acting in unfractured ice at the same level below the surface, so that,

$$2K + P = \rho g d + P$$

and $$d = 2K/\rho g, \text{ as before.}$$

It is conceivable that where the thickness of the ice is not very great compared with $2K/\rho g$, and in places of high velocity and of excess bending, crevasses could open up to depths exceeding this theoretical depth, which pertains to a slab of ice moving down a uniform slope.

A departure is now made from the perfectly plastic case. Nye (1955) uses a general flow law of the type derived by Glen (1952) to express the yield stress in tension in terms of the strain rate. At the point of failure of the ice at the surface $\sigma_x = \sigma_c$ so that the depth of fracture can be expressed as:

$$d = \frac{\sigma_c}{\rho g} = \frac{1}{\rho g}\left(\frac{\dot{\epsilon}_c}{B}\right)^{\frac{1}{n}} \qquad (5)$$

where $\dot{\epsilon}_c = B\sigma_c^n$ provides the relationship between stress and strain rate. $\dot{\epsilon}_c$ can be measured at the surface. Certain complications arise however, in selecting the appropriate value of strain rate. This will

be discussed later under Field Data Reduction and Results. Meyerhof (1954) gives some further ideas on crevasse depths but because the theory is based on soil mechanics the applicability of it to the present problem is very doubtful.

Extending and compressive flow

It is instructive to review certain concepts that help to define the terms "extending" and "compressive" flow, which were introduced by Nye (1952). The term "compressive" should be replaced by "contracting" to be consistent, but the original term will be used here because of its extensive use in the literature.

If $\dot{\epsilon}_x > 0$ in any region of the glacier then that region is one of "extending" flow.

If $\epsilon_{xx} < 0$ then a state of "compressive" flow is recognized.

By reconsidering the model used by Prandtl (1923), it is possible to determine the form of the loci of maximum shear stress within the plastic material. Because the same solution is obtained irrespective of slope and mass considerations, it is convenient to regard the behavior of a weight-less perfectly plastic material being compressed between parallel plates. As before, the lower half of the model is intended to represent a glacier at the centerline of flow.

The stress solution for a point within the material is given by:

$$\sigma_x = \frac{kx}{h} \pm 2k\sqrt{1 - z^2/h^2} + p$$

$$\sigma_z = \frac{kx}{h} + p$$

$$\tau_{xz} = -\frac{kz}{h}$$

where z is measured vertically from the median plane of the slab. At any point (x, z), the slope of the maximum shear stress curve is given by

$$\frac{dz}{dx} = \tan\left(\frac{\pi}{4} - \lambda\right)$$

where λ is the angle between the x axis and one of the principal stress axes.

By using Mohr's circle of stress and placing $\sigma = \frac{1}{2}(\sigma_1 + \sigma_2)$ the components of stress are expressed:

$$\sigma_x = \sigma + K\cos 2\lambda$$

$$\sigma_z = \sigma - K\cos 2\lambda$$

$$\tau_{xz} = K\sin 2\lambda$$

From this, dz/dx can be expressed as

$$\frac{2(K - \tau_{xz})}{\sigma_x - \sigma_z}$$

for extending flow.

The orthogonal set of maximum shear stress "trajectories" possess slopes given by

$$-\frac{\sigma_x - \sigma_z}{2(K - \tau_{xz})}$$

Substituting for σ_x, σ_z and τ_{xz} in terms of h and z, and integrating, it can be shown for the first case that

$$x = h\left\{\sin^{-1}\frac{z}{h} - \frac{\sqrt{h^2 - z^2}}{h}\right\} + c$$

which is the equation of a family of cycloids.

At z = -h the planes of maximum shear stress approach the bed tangentially; the orthogonal set exists even if it has no physical manifestation.

In the case of extending flow, the maximum shear stress planes that dip downstream and are tangential to the bed, are of prime importance. Because crevasse depths are only about four percent of the total ice thickness on the North Arm of Kaskawulsh Glacier, it is not expected that these fractures will have much noticable effect on regional stress patterns, which have just been considered.

Nye (1951, p. 567) has reported the occurrence in an alpine glacier of what he recognizes as shear fractures caused by shear plane slip in a zone of extending flow. Bull (pers. comm.) reports that these phenomena also occur in the accumulation areas of "cold" glaciers. However, these structures are not commonly observed and it is possible that their surface manifestation is often obscured by frequent snow accumulation in the upper regions of the glacier. The presence of such fractures would tend to reduce the immediate possibility of crevasse formation, since locally, stresses have been relieved.

In compressive flow, however, planes dipping up glacier at 45^{o} to the surface and approaching the bed tangentially assume importance. Occurrences of overthrust planes are commonly reported in the literature (e.g. Lewis, 1949).

Surface stress distribution

Consideration will be given to the two dimensional stress field existing in the plane of the glacier surface. The model considered is a valley ice stream of constant-width, although different "boundary conditions" are included in the analysis. Further assumptions are that the ice depth is small compared with the width and that the surface is

horizontal, so that gravity effects can be ignored. This is a good approximation in the case of the North Arm of Kaskawulsh Glacier since slopes do not exceed 2^{o} in the area studied.

Rectangular reference axes are adopted so that the x-axis points down glacier along the central flow line and the y-axis is transverse, in the plane of the surface. Consider σ_x , σ_y , and τ_{xy} to be the only stresses acting in the system. The effect of normal air pressure does not alter the analysis. By considering certain combinations of these stresses, depending on whether the flow is extending or compressive and depending on the type of boundary conditions, the magnitude and direction of the principal stresses at any point may be found, by using a Mohr's circle construction.

Nye (1952, p. 91) is able to explain the occurrence of three basic types of crevasses, only one of which is relevant here. Nielsen (1958) considers other combinations of stresses in order to cover all possible cases but nothing basically new is presented.

To explain transverse creavasse patterns, it is necessary to consider the state of extending flow, namely that $\sigma_x > 0$ over the length of glacier considered (Figure 5-A).

σ_y is controlled by the boundary conditions. According to the theory of plasticity developed by Hill (1950), $0 \leq |\sigma_y| \leq |\frac{1}{2}\sigma_x|$ where the maximum value of σ_y occurs when lateral contraction of the ice is prevented.

τ_{xy} varies from a maximum at the boundaries to zero at the center-line of the ice stream.

By considering values of σ_x , σ_y , and τ_{xy} at points in the x,y plane, a Mohr's circle construction gives, in each case, the magnitude and orientation of the principal stresses (Figure 5-B and 5-C). Assuming that the fracture occurs perpendicular to the direction of principal tensile stress, it is possible to plot the fracture trace. Figure 5-D shows the plot for a transverse creavasse system.

If transverse contraction is prevented there is a certain value of τ_{xy} for which both principal stresses are tensile. Thus, if $\sigma_y \leq \frac{\sigma_x}{2}$ and $\sigma_2 \geq 0$, Figure 5-E shows that $\tau_{xy} = \sigma_x/\sqrt{2}$. This condition is confined to central zone of the glacier, as is shown in Figure 5-D.

In real glaciers the idealized pattern of crevasses may be somewhat distorted by irregular boundary conditions, differential surface velocities and anisotropy of the ice. In the case of the Kaskawulsh Glacier transverse crevasses, a close correspondence with the theoretical pattern is noted. No longitudinal fractures occur, however. Down glacier, differential surface velocities cause a straightening of the traces, and later, a convexity downstream.

Consideration of Longitudinal Strain Rate

It is necessary now to analyze the conditions which contribute toward the states of extending or compressive flow within a body of ice moving downslope under the action of gravity and certain boundary conditions. Nye (1951, 1952, 1959a, 1959c) has developed the theory which follows. In this, the effects of various physical factors are analyzed separately and the principle of superposition is used to combine the

component strain rates. Certain simplifying assumptions are made. Ice is considered to be a perfectly plastic material, the shear stress on the bed is considered constant and the longitudinal strain rate is considered invariant with depth, or

$$\frac{\partial \dot{\epsilon}_x}{\partial z} = \frac{\partial}{\partial z}\left(\frac{\partial u}{\partial x}\right) = 0 \tag{6}$$

Consider the effect of accumulation or ablation at the surface of a glacier. Let $a = \frac{dq}{dx}$ be the rate of addition or subtraction of material at the surface of the glacier. A positive sign is used for accumulation, a negative sign for ablation. For simplicity a is assumed to be a constant rate for a yearly period. So that an equilibrium ice thickness can be maintained it is necessary for a longitudinal strain rate of $\frac{1}{h}\frac{dq}{dx}$ to exist. A positive $\frac{a}{h}$ term favors extending flow while a negative term favors compressive flow.

Next, consideration will be given to a glacier moving over a bed of variable slope. It is required, however, that $\frac{d\alpha}{dx}$ and $\frac{d\kappa}{dx}$ are small. By considering curvilinear coordinates (x, z) with reference to the bed surface it can be shown that the longitudinal strain is given by $\frac{q}{hR}\cot\alpha$, where q/h can be represented by a mean velocity $\bar{V}_c$ and hence the expression can be rewritten as

$$\bar{V}_c \kappa \cot\alpha \tag{7}$$

There has been some inconsistency in defining κ. Nye (1951, 1957b, 1959a) states that κ refers to the surface curvature but in other papers (1952, 1959b, p. 400) κ is associated with bed curvature. In the derivation of $\bar{V}_c \kappa \cot\alpha$, κ and α are associated with the same surface; this fact should be noted.

A slightly different method of derivation will now be used to obtain the above two expressions, $\frac{a}{h}$ and $\bar{V}_c \kappa \cot \alpha$, representing longitudinal strain rate. In addition, further terms will be added by superposition. These ideas were presented by Nye (1959b).

Consideration will be given to a glacier moving partly by internal differential motion and partly by bed slip. The assumptions made at the beginning of this section will be modified. Ice is not, now, assumed to be perfectly plastic and allowance is made for variations of shear stress on the bed of the glacier. The value of n in the flow law is considered to be finite and a relationship of the form,

$$V_b = \left(\frac{\tau}{B}\right)^m$$

is assumed to hold at the bed of the glacier. $\dot{\epsilon}$ is then expressed as $\frac{\partial V_b}{\partial x}$ and this is assumed to be constant throughout the thickness. Nye (1959c), Paterson (1962) and others state that $\dot{\epsilon}_x$ can vary with depth, but for simplicity of analysis, the assumption is used. Since $\tau = \rho g h \sin\alpha$, the longitudinal strain rate $\dot{\epsilon}_x$ can be written

$$\dot{\epsilon}_x = \frac{\partial V_b}{\partial x} = \frac{\partial V_b}{\partial \tau} \frac{\partial \tau}{\partial \alpha} \frac{d\alpha}{dx} + \frac{\partial V_b}{\partial \tau} \frac{\partial \tau}{\partial h} \frac{dh}{dx}$$

from which,

$$\dot{\epsilon}_x = m V_b \kappa \cot \alpha + \frac{m V_b}{h} \frac{dh}{dx}$$

where $$\kappa = \frac{d\alpha}{dx} \cdot$$

It is now necessary to consider at any given point the change in height of the ice surface with respect to time. $\frac{\partial h}{\partial t}$ can be expressed in terms of three components. The first term is a or $\frac{dq}{dt}$ measured

positive if accumulation, negative if ablation. It is also assumed to be a uniform rate of accumulation or ablation.

If the velocity components, respectively parallel and perpendicular to the ice surface be denoted by u_s and v_s then the vertical component of velocity is $v_s - u_s \frac{dh}{dx}$, being positive in an upward direction. It is noted that for mild slopes the vertical component of v_s is for practical purposes just v_s.

The total effect is obtained by addition of terms so that

$$\frac{\partial h}{\partial t} = a + v_s - u_s \frac{dh}{dx} \tag{8}$$

Considering now a three-dimensional strain rate system, the longitudinal strain rate can be related to the transverse and vertical strain rate thus: $\dot{\epsilon}_x = -(\dot{\epsilon}_y + \frac{v_s}{h})$ assuming incompressibility. Hence, $\dot{\epsilon}_x$ can be expressed as

$$m V_b \kappa \cot\alpha + \frac{m V_b}{h} \cdot \frac{1}{u_s} \left(a - h\{\dot{\epsilon}_x + \dot{\epsilon}_y\} - \frac{\partial h}{\partial t}\right),$$

which reduces to

$$\dot{\epsilon}_x = \frac{m V_b}{m V_b + u_s} \left(\frac{a}{h} - u_s \kappa \cot\alpha - \dot{\epsilon}_y - \frac{1}{h}\frac{\partial h}{\partial t}\right).$$

Nye, (1959c, p. 506) expresses $\dot{\epsilon}_y$ as $\frac{\bar{v}}{W}\frac{dW}{dx}$ but since this is the average value for the whole glacier cross-section it appears more appropriate to use the value of $\dot{\epsilon}_y$ measured near the center line of flow. However, as Nye has pointed out (pers. comm.), this ignores any variation of $\dot{\epsilon}_y$ with depth.

Consideration will now be given to an effect of bending of the ice. Simple elastic bending is assumed. Taking curvilinear coordinates (x, z) on the neutral plane of bending so that z is perpendicular to this plane, the strain increment is given by $d\epsilon_x = z\,d\kappa$ at a distance z above the neutral plane. From this, $\dot{\epsilon}_x = z\frac{d\kappa}{dt} = z\nabla\frac{d\kappa}{dx}$.

If it is assumed that the neutral plane is midway through the thickness then on the upper surface,

$$\dot{\epsilon}_x = \tfrac{1}{2} h \bar{\nu} \frac{d\kappa}{dx}$$

It should be noted that the value of this bending term changes with depth, but since the surface strain rate is being studied this fact does not affect the argument. The final equation can be written as

$$\dot{\epsilon}_x = \frac{m V_b}{m V_b + U_s} \left(\frac{a}{h} + U_s \kappa \cot\alpha - \frac{1}{h} \frac{\partial h}{\partial t} - \dot{\epsilon}_z + \tfrac{1}{2} h \bar{\nu} \frac{d\kappa}{dx} \right) \qquad (9)$$

The coefficient $\frac{m V_b}{m V_b + U_s}$ thus modifies the relation by using results of the experimental flow law for ice.

A numerical value may be assigned to this coefficient by considering typical values of m, V_b and u_s. If plug-flow is assumed (see Nye, 1952, p. 83) for a value of m = 2.5 for temperate ice, the coefficient has a value of 0.7. For a condition in which u_s is composed of equal contributions from bedslip and internal movement, the coefficient is 0.6. Judging by vertical velocity profiles in similar glaciers it is considered probable that the coefficient is of the order of 0.65 for this section of Kaskawulsh Glacier.

Crevasse Spacing

There is a paucity of general information bearing on the problem of crevasse spacing. Approaches to the problem have either been empirical or else analytic but of doubtful validity. Meier and others (1957) find by field measurements in Greenland that the spacing of certain crevasses is roughly four times the mean crevasse depth. However, these were not

true transverse crevasses. Nielsen (1958) claims to provide an explanation for the uniformity of crevasse spacing. However, the data from Kaskawulsh Glacier does not suggest a uniformity in spacing (Figure 6).

Nielsen (1958) considers a flowing cantilever ice slab, which, on attaining an unsupported length s fractures in elastic bending. If the ice thickness is h and the bending strength is S then it can be shown that

$$s^2 = \frac{Sh}{3\rho g} \tag{10}$$

Nielsen uses a value of 13.6 kg.cm.$^{-2}$ for the bending strength and finds that computed values of s are too great by a factor of 4, compared with field measurements of s. Now although some suggestions are made to explain the inappropriate value of S, no recalculation of s is made. Some laboratory tests on the bending of melting ice beams made by Neronov (in SIPRE Report 4, 1951, p. 24) yielded an average value of S of 4 kg.cm.$^{-2}$. It should be pointed out that the value of S is considerably lower in the upper regions of a glacier where snow and firn are the predominant materials. To counteract this effect in the equation for s, it must be noted that the average value of ρ is lower. Thus, the value of S/ρ is important.

Because the model used by Nielsen does not faithfully reproduce the probable conditions in a real glacier, his approach may be open to some criticism. A similar approach to the problem could be repeated using recent plastic theory for determining the bending moment in beams. However, from general observations of the formation of crevasses (Nielsen, pers. comm.) it may be thought more appropriate to use elastic theory.

Another approach to the problem is to consider the conditions occurring near the uppermost crevasse of a set of transverse crevasses.

Consideration will be given to the process of fracture taking place on the "dynamic" centerline of flow. Across the crevasse, $\sigma_x = 0$. As the crevasse moves down glacier the longitudinal stress reaches the critical value σ_c , and another crevasse is formed. Before the point of failure, however, there must exist a gradient of stress, and hence of strain rate. The local stress supposedly varies in some manner from zero to the critical value in a distance s, measured up glacier from the crevasse which has recently moved away from its point of origin. If a linear variation of stress is assumed as a first approximation, then

$$\frac{\partial \sigma_x}{\partial x} = \frac{\sigma_c}{s} \quad ,$$

so that

$$s = \sigma_c \Big/ \frac{\partial \sigma_x}{\partial x}$$

Now

$$\sigma_x = \left(\frac{\dot{\epsilon}_x}{B}\right)^{\frac{1}{n}} \qquad \text{from the flow law,}$$

$$\frac{\partial \sigma_x}{\partial x} = B^{-\frac{1}{n}} \frac{\partial \dot{\epsilon}_x^{\frac{1}{n}}}{\partial x} \quad .$$

Previously, an expression (9) was derived for $\dot{\epsilon}_x$ at a point on the surface, but rather than to differentiate this equation, it is obviously simpler to use direct measurements of $\dot{\epsilon}_x$, in order to obtain the value of $\frac{\partial \dot{\epsilon}_x^{1/n}}{\partial x}$.

Where $\dot{\epsilon}_x = \dot{\epsilon}_c$, the spacing is given by

$$s = (\dot{\epsilon}_c)^{1/n} \Big/ \frac{\partial \dot{\epsilon}_x^{1/n}}{\partial x} \quad . \qquad (11)$$

It seems probable that crevasse spacing is, at least in part, influenced by crevasse depth. At the edge of an ice sheet in north-east Greenland, Meier and others (1957) found that certain unclassified

crevasses having depths, d, of from 22 to 26 meters possessed spacings of about 4d. Kaskawulsh Glacier transverse crevasses are separated on an average by 2.8d where d ranges from 24 to 26 meters. It should be noted however, that these are not similar types of crevasses and the morphologies of the two glaciers are much different. To approach the problem in a more rigorous manner it will be necessary to examine the stress distribution with depth and distance up glacier from a forming crevasse.

FIELD METHODS

General Introduction

Previous investigators working in this area have included topographic surveyors, geophysicists and glaciologists. Triangulation and topographic observations were carried out by Wood in 1961 (Wood, 1963), snowpit stratigraphy and general glaciological studies were undertaken by Ragle during 1961 to 1963 (in Wood, 1963), ice velocity determinations were made by Zysset in 1962 and by Sharni (1963) while geophysical measurements were conducted by Clarke in 1963.

In 1964 existing triangulation stations were used but certain extensions were made (Brecher, 1965). Figure 2 shows the configuration of triangulation points and glacier stations.

The gravity survey was made in 1964 because it was considered that the gravity and seismic results of Clarke could be improved. Gravity and seismic data, respectively, suggested that the ice thickness at Station 4 was 575 and 740 meters (Clarke, pers. comm.). It is now known that the gravity traverse was not closed on bedrock and that the delay time used in the interpretation of seismic data was overestimated, thus in the latter case, giving lower values of ice depth. Thus it was considered that a gravity traverse across the glacier should be repeated.

Four types of surveys were undertaken in 1964; these are now discussed.

Velocity Distribution Survey

A study of short term glacier motion was undertaken by Mr. H. Brecher. For this purpose, twenty-one 4-meter bamboo poles were established on the surface of the glacier on three transverse lines (Figure 7). A pre-existing longitudinal line of metal poles was resurveyed to provide additional data.

The positions of these markers were determined by five surveys involving intersection and resection observations. These data were used for an analysis of surface ice velocities (Brecher, 1965). Velocities computed for the period 21 July to 14 August were used for determining the strain rate field in the region of the crevasses.

Instruments used were Wild T2 360^{o} and 400^{G} theodolites. Detailed survey procedures will be found in Brecher (1965).

Strain Net Survey

Three strain diamonds of 200-meter diagonals were established on markers 1, 2, and 3 (see Figure 2). Corner markers were 1.5 meters long, 2.5 cm diameter bamboo poles which were initially placed with about 0.33 meter above the glacier surface. As the ablation season continued these poles had to be reset frequently.

Three surveys of these diamonds were made with a 100-meter steel tape. All sides and diagonals were measured by flat chaining under standard tension. Snow surface and air temperature measurements were made and a corresponding temperature correction was calculated. The position of the central marker was determined by resection. The internal angles of

each strain diamond were determined. Surface slopes were also measured. More detailed descriptions of similar surveys are given in Nye (1959b).

Gravity Survey

Measurements of gravity were carried out by Dr. C. Bull using a Worden Master gravimeter, geodetic model. This survey was made along a transverse profile between Stations H and K (Figure 2) where seven 6-meter metal poles remaining from the seismic survey of Clarke in 1963 served as convenient gravity stations as well as velocity markers. The position of gravity stations was determined by resection. For more detailed descriptions see, for example, Bull and Hardy (1956).

Crevasse Survey

Theodolite resections, taping, and compass bearings were used to plot the set of crevasse traces. Within the crevasses, Brunton compass and taping techniques were used to determine the configuration of the interior. Surveyor's steel arrows were used as markers for measurements of vertical strain rate and crevasse opening rates. Crevasses were descended by means of a 30 meter wire ladder anchored to ice pitons and bamboo poles embedded in the firn. Plate 6 shows the ladder in position within a crevasse.

Field travel was facilitated by the use of motor toboggans and skis.

FIELD DATA REDUCTION AND RESULTS

Velocity Determination

Survey data were reduced by Mr. H. Brecher using computer techniques (Brecher, 1965). Gravity station positions, which also provided velocity data, were computed using a desk calculator. The velocity vector field was determined over a 25-day period in July and August. Figure 7 shows a construction of flow-line filaments which are assumed to be a family of smooth curves.

Adopting the rectangular axes (X, Y) established by Wood in 1961, contour diagrams of V, V_X and V_Y have been constructed (Figures 8, 9, and 10). A discussion of the accuracy of velocity measurements is given by Brecher (1965).

An estimate of the mean flow velocity over the depth and width, and of the ice throughflow between H and K has been made. A value of mean surface velocity $\bar{V}_s$ for the transverse profile between Stations H and K, was obtained using standard semigraphical methods. Generally $\bar{V}_s \simeq 0.85\ V_c$.

It can be shown that

$$\frac{\bar{V} - V_b}{\bar{V}_s - V_b} = \frac{n+1}{n+2}$$

(Nielsen, 1955 and Paterson, 1962)

Assuming that $V_b \simeq 0.25\ V_s$, (although it may reach $0.50\ V_s$ in some temperate glaciers) and putting n = 3.17 (Glen, 1953, p. 721; 1955, p. 528) a value of $\bar{V}$ is obtained. Since these velocities pertain to a yearly period, the time unit, 1 year, will be retained. A value of 71.8 $m.yr.^{-1}$ is obtained for the mean ice velocity $\bar{V}$, between H and K.

An estimate of ice throughflow between H and K is obtained from a knowledge of the cross-sectional area of ice measured from Figure 5. A value of $Q \simeq 116.3 \times 10^6$ m.^{3} yr.$^{-1}$ is obtained. The throughflow of ice per unit width in the region of the median flow plane at Marker 4 is $q_4 \simeq 67 \times 10^3$ m.^{2} yr.$^{-1}$.

Short term surface velocity measurements (Brecher, 1965) indicate that surface ice velocity fluctuations, if they exist, must be less than 10 or 15 percent for weekly periods during the summer season. Comparison of velocities over longer time periods indicate that variations decrease.

Regional Strain Rate Computations

Three main methods have been used for determining the strain rate tensor on the surface of the glacier.

(a) Velocity gradient method. At convenient points on Figures 9 and 10 values of $\frac{\partial V_x}{\partial X}$, $\frac{\partial V_x}{\partial Y}$, $\frac{\partial V_Y}{\partial X}$, and $\frac{\partial V_Y}{\partial Y}$ were obtained by semigraphical methods.

Thus, at each point the components of strain rate were determined from

$$\dot{\epsilon}_x = \frac{\partial V_x}{\partial X}$$

$$\dot{\epsilon}_Y = \frac{\partial V_Y}{\partial Y}$$

and

$$\dot{\gamma}_{xY} = \frac{\partial V_x}{\partial Y} + \frac{\partial V_Y}{\partial X}$$

The principal strain rate tensors $\dot{\epsilon}_1$ and $\dot{\epsilon}_2$ have been obtained using a Mohr's circle construction such as is shown in Figure 5-B. Figures 11, 12, and 13 show contours of the principal strain rate components.

Certain assumptions have been made in the foregoing analysis. These will be mentioned briefly.

1. The surface of the glacier is assumed to approximate a horizontal plane. This is a good approximation since surface slopes do not exceed 2^{o}.

2. Plane strain is assumed. The effect of normal air pressure does not alter the analysis.

3. Strains are assumed to be continuous functions of X and Y, so that regional or average values of strain rate are obtained.

4. Strains are small enough to produce no serious elliptical distortion of Mohr's circle.

(b) Strain diamond method. Methods of data reduction were the same as those given by Nye (1959b). Measured lengths for each strain net have been corrected for temperature, slope, and height above sea level. The maximum probable error in the length measurements is estimated as 1 in 20,000. This estimate includes possible movement of corner markers.

The components of strain rate were computed from

$$\dot{e} = \frac{2.3}{\Delta t} \log_{10} \frac{l_2}{l_1}$$

which is a more exact and easier to use expression than

$$\frac{1}{\Delta t} \cdot \frac{\Delta l}{l_1}$$

Rectangular axes x', y' are now chosen so that the x' axis coincides with the longitudinal diamond diagonal on which $\varphi = 0^{o}$. Rotation of the diamonds was negligible and the x', y' axes very nearly coincide with the x, y axes. The z' axis is perpendicular to the x' and y' axes.

$\dot{\epsilon}_{o}$, $\dot{\epsilon}_{45}$, $\dot{\epsilon}_{90}$, and $\dot{\epsilon}_{135}$ have been measured and theoretically, from geometrical considerations.

$$\dot{\epsilon}_{o} + \dot{\epsilon}_{90} = \dot{\epsilon}_{45} + \dot{\epsilon}_{135}$$

the subscript corresponding to the values of φ.

It is required to deduce the best values of $\dot{\epsilon}_{x'}$, $\dot{\epsilon}_{y'}$, and $\dot{\gamma}_{x'y'}$ referred to the center of the strain diamond. Nye (1957a) by using matrix methods, shows that the best values of the strain rate components are

$$\dot{\epsilon}_{x'} = -\tfrac{1}{4}\dot{\epsilon}_{o} + \tfrac{1}{4}\dot{\epsilon}_{45} + \tfrac{3}{4}\dot{\epsilon}_{90} + \tfrac{1}{4}\dot{\epsilon}_{135}$$

$$\dot{\epsilon}_{y'} = \tfrac{3}{4}\dot{\epsilon}_{o} + \tfrac{1}{4}\dot{\epsilon}_{45} - \tfrac{1}{4}\dot{\epsilon}_{90} + \tfrac{1}{4}\dot{\epsilon}_{135}$$

and $$\dot{\gamma}_{x'y'} = \dot{\epsilon}_{45} - \dot{\epsilon}_{135}$$

Also,

$$\dot{\epsilon}_{z'} = -(\dot{\epsilon}_{x'} + \dot{\epsilon}_{y'})$$ assuming incompressibility.

The principal strain rates are now either obtained from a Mohr's circle construction or else computed directly from

$$\dot{\epsilon}_{1} = \tfrac{1}{2}(\dot{\epsilon}_{x'} + \dot{\epsilon}_{y'}) - \left\{\tfrac{1}{4}(\dot{\epsilon}_{x'} - \dot{\epsilon}_{y'})^{2} + \tfrac{1}{4}\dot{\gamma}^{2}_{x'y'}\right\}^{1/2}$$

$$\dot{\epsilon}_{2} = \tfrac{1}{2}(\dot{\epsilon}_{x'} + \dot{\epsilon}_{y'}) + \left\{\tfrac{1}{4}(\dot{\epsilon}_{x'} - \dot{\epsilon}_{y'})^{2} + \tfrac{1}{4}\dot{\gamma}^{2}_{x'y'}\right\}^{1/2}$$

The orientation of the axes is given by

$$\tan 2\theta = \frac{\dot{\gamma}_{x'y'}}{\dot{\epsilon}_{x'} - \dot{\epsilon}_{y'}}$$

Using methods outlined by Nye (1959b, p. 413) the residuals δ of the measured values $\dot{\epsilon}_0$, $\dot{\epsilon}_{45}$, $\dot{\epsilon}_{90}$, and $\dot{\epsilon}_{135}$ are found. $|\delta|$ is the difference between the measured value $\dot{\epsilon}_y$ and the adjusted value. The standard error in $\dot{\epsilon}_{x'}$ and $\dot{\epsilon}_y$ is $\sqrt{3}|\delta|$ which is about

$$\pm 0.05 \times 10^{-5} \text{ day}^{-1}.$$

Figure 14-A shows the strain rate field in the region of the crevasses.

(c) Approximate values of longitudinal strain rate have been obtained using the four velocity markers which had been surveyed in 1963 and 1964. The values of strain rate obtained from this strain line are shown in Figure 14-B. Other estimates of strain rate have been made using the relation $\dot{\epsilon}_{xc} = \frac{\dot{W}_c}{S}$. These results are shown in Figure 15-A, B, C, and indicate that the previous assumption that the strain is taken up by opening or closing of a crevasse is a reasonably good one.

Estimate of critical strain rate.

Figure 11 shows contours of principal extending strain rate. By overlaying this plot on the map of crevasse traces it is possible to estimate a value of strain rate associated with fracture of the ice. The strain diamond at Marker 3 records a strain rate very close to $\dot{\epsilon}_c$. An approximate regional value of $\dot{\epsilon}_c$ has thus been deduced as 3.5×10^{-5} day^{-1}, $\pm 0.5 \times 10^{-5}$ day^{-1}.

Meier and others (1957) and Meier (1960), from observations in Greenland and on Saskatchewan Glacier, suggest a value of about 1% yr.$^{-1}$ (2.8×10^{-5} day^{-1}) while Mellor (1964) considers a value of 10^{-9} sec^{-1} (8.7×10^{-5} day^{-1}) to be of roughly the correct order. Neither of the two sources states the strain rate gradient which is associated with

the critical values, but it is considered important here. A regional gradient of about 0.005×10^{-5} day^{-1} m^{-1} is associated with the regional value of 3.5×10^{-5} day^{-1} for the critical strain rate.

It should be noted that great difficulty was experienced in determining the position of the uppermost crevasse. At the beginning of the summer it was considered that crevasses were forming just upstream of Marker 2 and hence the uppermost strain diamond was established at Marker 3. Later in the season an aerial observation showed that crevasses were forming almost up to Marker 3. Plate 3 shows a series of firn cracks upstream of Crevasse Camp.

It has been assumed for simplicity that the derived strain rates apply to a particular point although, due to ice movement of the order of 10 meters in 35 days, this is not strictly true.

Gravity Survey Computations

The survey was designed to provide data from which a cross-section of the glacier between Stations H and K could be calculated. An aim of prime importance was to determine a reliable value for ice thickness at the center-line of flow.

It has been mentioned under Field Methods that the metal poles used by Clarke in 1963 were used again in 1964. Since the maximum down glacier displacement of the poles is about 110 meters and since the bedrock gradient is less than 4^{o}, it is considered that a comparison between Clarke's ice thickness results and the 1964 results is justifiable.

Standard methods of reduction of the data were followed (e.g. Bull and Hardy, 1956). Individual corrections to measured gravity will be

briefly discussed.

(1) The free air correction. Absolute heights referred to mean sea level are probably within 5 meters; relative height differences for stations in the traverse are estimated to be within 15 centimeters.

(2) The Bouguer correction. Since the south side of the glacier is flanked by granodiorite and basic intrusions while limestones and dolomites and acid intrusions outcrop to the north, it is not known with any certainty how to give weight to the respective rock densities of 2.6 to 2.8 gm.cm.$^{-3}$ (Dobrin, 1960). From geological considerations and considering the approximate transverse profile of Clarke it is thought probable that sedimentary material underlies most of the glacier in this section.

Thus a "weighted" value of $\rho_{ROCK} = 2.65$ gm.cm.$^{-3}$ has been used, although towards Station K this becomes less accurate. At Station K a value of 2.8 gm.cm.$^{-3}$ was used.

(3) Topographic correction. This is the most difficult to analyze. An approximate bedrock profile can be obtained using the ice depth values which Clarke determined by gravimetric and seismic methods. Now by using data and graphs such as presented in Russel and others (1960) and Theil and others (1957) a reasonable approximation for the topographic correction was obtained. At the central station a correction of 3.65 milligals was used.

Since Stations H and K were over four kilometers apart the International Gravity Formula:

$$G_\phi = 978.0490 \left(1 + 0.0052884 \sin^2\phi - 0.0000059 \sin^2 2\phi \right) \text{ cm.sec.}^{-2}$$

was applied, and a linear variation of G_{ϕ} assumed between H and K. Estimated error in absolute station position is 15 meters. Relative position errors should not exceed ± 30 centimeters.

Coordinates for Station K were obtained from the map of the Icefield Ranges, scale 1:30,000 (Published by the American Geographical Society, New York, 1963).

Assuming an ice density of 0.9 gm.cm.$^{-3}$ the ice depth at Station 4 (1964) has been calculated as 635 meters, with an estimated error of 12-15 percent. Elsewhere ice thicknesses could be in error up to 20 percent. Figure 3 shows variously derived profiles.

The relative longitudinal bed profile determined by Clarke from seismic measurements has been adopted except that the absolute position has been readjusted to fit the new ice depth value at Station 4 (Figure 16).

Miscellaneous Computations

(1) Position determinations. Resection observations were made to locate gravity stations and some crevasses. Positions were determined by using a elegant method described by Clark (1957, p. 642).

(2) Crevasse dimensions are referred to a particular date and opening rates are referred to the period August 5 to August 13.

(3) Calculations of vertical strain rate have not been possible since these data and other minor material were lost in a crevasse.

(4) Shear stress calculations. The average shear stress on the bed has been obtained from a knowledge of the shape of the ice mass in the section between Stations H and K. For a glacier stream of constant

or slowly varying cross-section, Nye (1952) has shown that the average value of shear stress on the bed is given by

$$\tau_b = \rho g \frac{A}{p} \sin\alpha$$

Using the value of A obtained by planimeter and a value of p measured directly from the section in Figure 3,

$$\tau_b \simeq 0.85 \text{ bar.}$$

By using the expression derived for a semi-infinite sheet, namely $h = \frac{\tau_b}{\rho g} \operatorname{cosec} \alpha$ on the median plane of flow, a value of

$$\tau_b \simeq 1.4 \text{ bars}$$ is obtained.

Nye (1952) has found that the value of bed shear stress for sixteen alpine valley glaciers varies between 0.5 and 1.5 bars. Kanasewich (1963) shows that on a section of the Athabaska Glacier average shear stresses mostly vary between 0.8 and 1.1 bar with an average of 1.0 bar.

On Kaskawulsh Glacier only one cross-section has been determined but nevertheless, downstream of Station 4, considerable constriction of the ice flow takes place and the surface slope clearly has little direct relationship to the bed profile, so that the application of either of the above two expressions is considered untenable.

Accumulation and Ablation Data

Accumulation

As a result of observations of snow stratigraphy in pits and of pole measurements since 1961, reasonably reliable estimates of the mean net annual accumulation are available. Observations of snow stratigraphy on the haunch of a crevasse bridge provide values that agree tolerably

well with the values for previous years obtained by Ragle (pers. comm.). Below is a table which summarizes the data. Method of determination is by measurement on poles unless otherwise stated. Data other than that from the crevasse has been provided by Ragle (pers. comm.).

TABLE 1

Accumulation on the North Arm of Kaskawulsh Glacier

Pole Number See Figure 2	Mean Annual Net Snow Accumulation (cm Water Equivalent) 1961-62	1962-63	1963-64
1	--	106, 110†	103, 93†
2	--	130	123
3	--	143	141
4	129*	134	156
5	130*	146	168

* Pit determination
† Crevasse bridge (haunch) stratigraphy
Average snow density has been taken as 0.520 gm.cm.$^{-3}$.
Note that velocity of Pole 1 is approximately 0.430 m. day^{-1}.

There is clearly an accumulation gradient within the 1800 meters in which the observations have been taken. These data are used later in the computation of strain rates. The assumption is made, however, that this accumulation is a uniformly distributed loading rate throughout the year. This will be discussed later in the section.

Ablation

Although the ablation data are not used directly in computing strain rates the implications are worth noting (see next section on Discussion of Data and Results). Measurements of average surface lowering were taken

from velocity poles between July 7 and August 11, 1964. A mean value of 0.98 cm.day^{-1} was obtained for this period, but this contains the effect of densification as well as direct ablation. The densification, as estimated from a knowledge of the density profile is, for this short time period, negligible.

Wagner (1963, p. 42) estimates that for July and August, 1963, the average ablation in the region to the west of the crevassed area at altitude 2500-2600 meters was 0.8 to 0.9 cm.day^{-1}. The average surface density is about 0.410 gm.cm.$^{-3}$.

Use of data

The effect of accumulation or ablation on the longitudinal strain rate has been considered previously under Theoretical Considerations.

In the calculations of the $\frac{a}{h}$ term in equation (9), values of a lying between +0.32 cm.day^{-1} and +0.46 cm.day^{-1} have been used. The values are in terms of cm. of ice of density 0.9 gm.cm.$^{-3}$ assumed to be uniformly applied over the year. The effect of a negative $\frac{a}{h}$ term during the summer is considered in the Discussion of Data and Results.

Field Measurements of Crevasse Depths

General data

Field estimates of crevasse depths are many and variable. There are several reasons for this.

(1) Direct measurement by "plumbing" from the surface is hindered when the plumbing device becomes jammed before the crevasse terminates. Other pitfalls are evident. Sometimes substantial quantities of water are present in the bottom of the fracture.

(2) Crevasses that are in the process of closing mainly by plastic deformation at depth may be measured as shallower than the original depth.

(3) In fact, in view of the equation for $\dot{\epsilon}_x$, the bending term indicates that it should be possible to have σ_x tensile to a depth greater than that given by the idealized model, and so we expect a considerable range of depth values to be observed.

Nye, and others (1954) have discussed, generally, the depth of crevasses. Schuster and Rigsby (1954) state that observed crevasse depths are generally of the order of from 50 to 100 feet (15 to 30 m.) but may extend to 150 feet (50 m.) or more. According to Seligman (1955) most crevasses in the European alpine glaciers do not exceed 30 meters in depth but Loewe (1955, p. 511) cites a crevasse in the Bernese Oberland as being nearly 40 meters deep. This was at an altitude of 3700 meters. Goldthwait (1936) using seismic methods on part of Crillon Glacier, Alaska, estimated that crevasse depths averaged 20 meters. Miller (in Nye, 1955) reports that crevasses in some Alaskan glaciers average 30 meters. Taylor (1962) gives depth values of 10 meters for closing crevasses on part of Burroughs Glacier, Alaska. The author's observations on New Zealand glaciers are in general agreement with the above figures. Greenland and Antarctic crevasses have been reported as being up to 150 to 200 feet (45 to 60 m.) in depth. Such values may be explained by the change in the ultimate strength properties of ice with temperature and by the measurably slower increase of density with depth. Equation (5) shows the effect of these parameters on the depth d.

Kaskawulsh Glacier transverse crevasse depths

Five consecutive transverse crevasses were plumbed for depth. These values are comparable with the computed depths obtained from Equation (5). Measured values generally lay between 24 and 28 meters. The estimated accuracy of individual measurements is probably 5%.

Calculation of Crevasse Depths

Meyerhof (1954) actually obtains an expression which gives depths of from 23 to 46 meters but his methods are suspect since he uses the mechanics of soils. Using the expression developed by Nye (1955), namely Equation (5), an estimate of theoretical crevasse depth is obtained (Table 2). Data from Glen (1953, p. 721, and 1955, p. 519) provides appropriate values of B and n in Equation (5). Strain rate values across crevasses as well as regional values have been used to compute d in Table 2. The critical strain rate of 0.0128 $yr.^{-1}$ yields a value of d = 7 meters. Results are discussed later.

Field Observations of Crevasse Spacing

Measurements of crevasse spacing are plotted against position on the glacier (Figure 6). Where a lateral variation in spacing between two adjacent crevasses occurred the mean value of a perpendicular to the traces was taken. In some cases a 20 percent variation in s was recorded. In the area, Figure 6 shows that crevasse spacings vary from about 30 to 100 meters, with a mean of about 75 meters. A decrease in spacing appears to occur with increasing age of the crevasses. It is not known whether this apparent spacing gradient has any significance or not, although individual variations will be discussed shortly.

TABLE 2

Crevasse Depths

Crevasse No.	Mean Density gm.cm.$^{-3}$	T (°C)	B bar^{-n} yr^{-1}	n	$\dot{\epsilon}$ Across Crevasse (yr^{-1})	$\dot{\epsilon}_x$ Regional (yr^{-1})	d Calculated Using $\dot{\epsilon}$ Across Crevasse (m.)	d Calculated Using $\dot{\epsilon}_x$ (m.)	Measured	Remarks
6	0.70	0	0.17	3.17	1.6	0.020	30.5	8.1	23.5 - 24	--
7	"	"	"	"	1.5	0.022	29.8	8.2	26	--
8	"	"	"	"	1.7	0.025	31.0	8.6	25.5 - 26	--
9	"	"	"	"	2.1	0.032	32.0	9.3	28 - 28.5	Measured Value of d Suspect.
10	"	"	"	"	1.3	0.037	27.0	9.7	27	
14	"	"	"	"	0.8?	0.046	24.5?	10.1	26.5	$\dot{\epsilon}$ Across Crevasse Suspect.
18	"	"	"	"	--	0.053	--	10.8	25.0	

A re-examination of the major factors influencing fracture spacing may suggest a solution to the above problem. The gradient of surface stress appears to be of utmost importance. Assuming certain conditions, it has been shown earlier under Theoretical Considerations that

$$s \frac{\partial \sigma_x}{\partial x} = \sigma_c$$

Variations in σ_c may be attributed to variations in the bulk properties and physical condition of the ice. Changes in $\frac{\partial \sigma_x}{\partial x}$ are due to variations in the accumulation or ablation gradient and variations in velocity at any point which affect the strain rate and hence the strain rate gradient. Also to be considered is the rate of change of thickness of the ice downstream (see Equation (8)). The occurrence of thermal stresses, which may be of the same order of magnitude as mechanically induced stresses if the temperature changes are rapid enough, should also be considered. (see Appendix II).

To explain the lateral variation in spacing of any two crevasses it is necessary only to invoke lateral changes in bed profile and velocity gradient profile, and so forth. Moreover, lateral changes in ice properties should be more pronounced than longitudinal ones in this area since the constriction produces heavy fields of shear crevasses close to the boundaries.

To explain the gradient in the spacing down glacier (Figure 6) it is possible to appeal to a steady change in the sum of all components in Equation (9). In other words substantial changes in velocity, velocity gradients and precipitation or ablation gradients and so forth, for at least ten years are required. This is roughly the time

taken for Crevasse 19 to reach its present position, assuming that it formed in the region of the first crevasse observed recently and assuming a mean velocity of flow of 130 $m.yr.^{-1}$. The magnitude of velocity and accumulation changes required to explain the observations does not seem reasonable. In fact, within this area, specific observations concerned with detecting velocity fluctuations show no significant variations for summer flow or yearly flow, although observations have only been conducted over two years (Sharni, 1963; Brecher, 1965).

The problem seems best resolved by appealing to changes in structural properties of the ice and firn. Laboratory tests on the ultimate strength of ice (see for example SIPRE Report No. 4, 1951) commonly show variations of two hundred percent, and in some cases more. Thus, such a magnitude of variation of σ_c would be more than sufficient to account for the observed variations in s.

However, this solution does not include a convincing explanation of the apparent increase in spacing with decreasing age. The first solution apparently does this.

Bearing in mind what has just been said, it seems unnecessary to attempt to explain the apparent existence of two "sets" of crevasses seen in Figure 6, except for one fact. Whereas the crevasses associated with the narrow spacing (35 m.) are conformable in the width sequence (see Figure 15-C), suggesting a consecutive formation. Crevasse 18 is only 20 centimeters wide but flanked by crevasses at least 500 centimeters wide, both of which must have been formed years before. Thus we are forced to conclude that there has been significant strain on an intercrevasse block which would have had in this case an unbroken width

of 112 meters, which is considerably larger than any spacings observed. Thus it is concluded that the previous assumption that $\dot{\epsilon}_x = 0$, on an intercrevasse block is only valid for "average" values of spacings. This is well verified by applying the relation:

$$\dot{\epsilon} = \frac{\dot{w}_c}{s}$$

to Crevasses 4 to 8 (Figure 15-A). Strain rates thus derived are comparable to values obtained by other methods.

Hence it is concluded that strain is taken up by opening (or closing) of existing crevasses unless the spacing for some reason is large compared with the average spacing, in which case significant strain can occur.

Calculation of Crevasse Spacing

Using the formula given by Nielsen (1958, p. 47) and putting

$$h = 650 \text{ meters}$$

$$S = 2 \text{ kg.cm.}^{-2}$$

$$\rho = 0.70 \text{ gm.cm.}^{-3}$$

$$g = 981 \text{ cm.sec.}^{-2}$$

a value of $s \simeq 79$ meters is obtained, and this lies within the range of measured values, and is very close to the mean value.

Using the formula involving strain rate characteristics (Equation (11)) leads to some difficulties since the detailed local values of surface strain rate up glacier of the first crevasse are not available. Preliminary estimates indicate that the calculated spacing is an order of magnitude too large.

Thus more detailed strain measurements on the surface of a glacier (as well as within the glacier) need to be undertaken in the region up glacier from a forming crevasse.

Calculation of Theoretical Longitudinal Surface Strain Rate

Computed values of strain rate given by Equation 7 have been determined. Results are shown in Tables 3 and 4.

Table 5 summarizes all the strain rate data and compares calculated with measured surface $\dot{\epsilon}$ values.

Positions 1′ through 4 lie on the dynamic center-line of the glacier which is located in Figure 17. The dynamic or geophysical center-line has been selected on the basis of the symmetry of velocity and strain distribution data. The geographic center-line has been located on the basis of the physical configuration of the ice, and the position of the boundaries.

TABLE 3

Computation of $\bar{V}_c \kappa \cot\alpha$ From Surface Data

Point	$\bar{V}_c$	$\tan\alpha$	κ surface	$\bar{V}_c \kappa \cot\alpha$	$h\kappa$ *	Validity
4	0.320	0.030	0.625×10^{-5}	6.4×10^{-5}	0.004	valid
3′A	0.315	0.0264	3.0 x "		0.02	not valid
3′	0.329	0.0162	3.0 x "	high -ve values	0.02	"
2′A	0.342	0.0117	1.1 x "		0.007	"
2′	0.362	0.0086	0.5 x "		0.0033	"
1′A	0.389	0.0076	0.5 x "		0.0033	"
1′	0.405	0.0049	0.2 x "	-16.6×10^{-5}	0.0013	?

(For positions of points see Figure 17.)

TABLE 4

Computation of $\bar{V}_c \kappa \cot\beta$ From Bed Profile Data

Point	$\bar{V}_c$	$\tan\beta$	κ bed	$\bar{V}_c \kappa \cot\beta$	$h\kappa$ *	Validity
4	0.320	0.0926	1.5×10^{-5}	-5.18×10^{-5}	0.0099	valid?
3′A	0.315	0.0750	11.0 x "		--	not valid
3′	0.329	0.0350	5.0 x "	high -ve values	--	"
2′A	0.342	0.0325	5.0 x "		--	"
2′	0.362	0.0075	12.5 x "		--	"
1′A	0.389	0.0425	13.5 x "		--	"
1′	0.405	0.0775	13.0 x "		--	"

* It is required, that in order for $\dot{e} = \bar{V}_c \kappa \cot\alpha$ to be approximately valid

$$h\frac{d\alpha}{dx} << \frac{dh}{dx}$$

$$h\kappa << \alpha$$

Only at Point 4 does this approximately hold. Of all the strain rate components, $\bar{V}_c \kappa \cot\alpha$ is the most critical.

TABLE 5(a)

List of Component Strain Rates

Point	h (meters)	$\frac{a}{h}$	$\bar{V}_c \kappa \cot\alpha$	$\frac{\bar{V}}{W}\frac{dW}{dx}$	$\dot{\epsilon}_y$ (measured)	$h^{-1}\partial h/\partial t$ (approx. only)
4	660	0.70×10^{-5}	6.4×10^{-5}	-5.5×10^{-5}	--	-0.5×10^{-5}
3′A	670	0.64 "	--	-5.6 "	--	"
3′	670	0.64 "	--	-5.6 "	-9.1×10^{-5}	-0.5×10^{-5}
2′A	660	0.660 "	--	-5.4 "	-11.5 "	"
2′	660	0.56 "	--	-5.9 "	-10.2 "	-0.3×10^{-5}
1′A	660	0.49 "	--	-6.5 "	-12.0 "	"
1′	690?	0.46 "	-16.6×10^{-5}	-7.3 "	-14.4 "	"

TABLE 5(b)

Comparison Between Computed and Measured Strain Rates

Point	$\frac{1}{2}h\nabla\frac{\partial\kappa}{\partial x}$	$\dot{\epsilon}_x$ Calculated (surface slopes used)	$\dot{\epsilon}_x$ Calculated (bed slopes used)	$\dot{\epsilon}_x$ Measured (regional)
4	-0.12×10^{-5}	7.7×10^{-5}	0.5×10^{-5}	2.5×10^{-5}
3′A	"	--	--	2.5 to 2.8×10^{-5}
3′	-0.15x "	--	--	4.3 "
2′A	0.168 "	--	--	5.2 "
2′	0.39 "	--	--	10.2 "
1′A	0.1 "	--	--	11.0 "
1′	--	--	--	14.0 "

DISCUSSION OF DATA AND RESULTS

Discussion of Velocity Data

It is appropriate here to introduce some discussion of the seasonal behavior of the ice stream.

Few comprehensive studies of seasonal ice surface velocity variations are available. Paterson (1964) discusses variations in velocity of Athabaska Glacier. Brecher (1965) has attempted to analyse short term velocity measurements made on the North Arm of Kaskawulsh Glacier. He finds that in practically every case any possible velocity variation is obscured by the standard error in the velocity values at each point. This applies to weekly, monthly and yearly velocity measurements. Thus no definite statement can be made regarding the velocity characteristics of the glacier, except that if fluctuations in velocity do exist, they are small.

The sliding mechanisms of glaciers on their beds have been dealt with in some detail by Weertman (1957, 1964) and Kamb and LaChapelle (1964). Weertman attributes changes in surface velocity to changes in sliding velocity dependent on the amount of water present at the basal interface and on the existence of traveling waves in the basal water layer.

On the basis of this information it is appropriate to review temperature observations in the Upper Kaskawulsh Glacier. Ragle, (in Wood, 1963) has classified the divide area as subpolar but measurements

by Higashi and Shimizu during the summer of 1964 show that the 0^{o} C isotherm existed to 15 meters, thus indicating a temperate classification. Probably the geophysical nature is transitionary (also Ragle, pers. comm.).

Measurements by the author within several crevasses showed that the 0^{o} C isotherm prevailed to 24 meters and in mid-August 1964 most crevasses contained about 2 to 4 meters of water. The ice region in which this work was accomplished is therefore recognized as "temperate". For this reason an "average" value of V_b for temperate glaciers has been used in calculating $\bar{V}$ in the previous section on Field Data and Results.

Temperature variations of a seasonal nature could be important in influencing the amount of internal ice motion, but since yearly, seasonal, and weekly velocities have been examined and no pronounced variations are found, it is concluded that the penetration of the winter cold wave is probably shallow. In the cases where seasonal temperature variations are significant for most of the depth, the winter behavior is influenced by accumulation, producing extending flow, while lower temperatures tend to reduce the flow. In the summer, the reverse is the case, since ablation favors compressive flow while higher temperatures induce higher flow velocities. In this way seasonal ice velocity and strain rate fluctuations may be reduced.

It should be noted that approximate strain rates for the year 1963-64 agreed with values obtained during the 1964 summer (see Figure 14-B).

Discussion of Strain Rate Data

Accumulation effect

It has been noted that during the summer the a/h term is negative

but that such periods are neglected in order to simplify the calculations. To substantiate this the assumption might be made that the plastic response to the added winter-spring snow-load is still occurring during the following summer and that it is only slightly modified by the summer ablation. These ideas are only valid if the response time of the glacier is at least three months, which appears to be a good assumption. Nye (1960, 1963) discusses the response time of valley glaciers.

Curvature effect

In the present analysis this term has proved difficult to interpret. Mention has been made (under Theoretical Considerations) of the fact that confusion exists over the use of the term κ.

Theoretical derivations require that κ and slope α be referred to the same curved surface; therefore these terms should be referred either to the bed or the ice surface. Preference to the latter is given because of convenience.

In the derivation of the curvature term (Nye, 1951, p. 561) it can be shown that

$$\frac{dh}{dx} = -\frac{h}{R}\cot\alpha$$

and not only must

$$\left|\frac{dh}{dx}\right| \quad \text{and} \quad \left|\frac{h}{R}\right| << 1$$

but

$$\left|\frac{h}{R}\right| << \frac{dh}{dx}$$

or

$$|h\kappa| << \alpha$$

to a good approximation.

It has been demonstrated in the case of the present study that whether bed slopes or surface slopes are used this criterion is not fulfilled except in one case. On a plane surface, $\bar{v}_c \kappa \cot\alpha$ vanishes.

Transverse strain rate

It has been suggested that the measured values of $\dot{\epsilon}_y$ on the surface and lying on the central flow line should be used instead of the values derived from $\frac{\bar{v}}{w}\frac{dw}{dx}$ as suggested by Nye (1959b). To use the surface values means that any variation of $\dot{\epsilon}_y$ with depth is neglected, whereas $\frac{\bar{v}}{w}\frac{dw}{dx}$ takes account of this. However, since all the measurements in this case are restricted to the surface of the glacier the surface value of $\dot{\epsilon}_y$ is more appropriate.

Rate of ice thickness change

This term is positive if the surface at a point is rising with time. Since 1961 the surface of this section of the Kaskawulsh Glacier has lowered (see Figure 16) and hence the term is negative. The 1964 summer velocity data could not accurately provide an estimate of $\frac{\partial h}{\partial t}$ and hence the results for the years 1962-63-64 have been averaged. This is a small term, and is approximate only.

Bending effect

This is the true bending term which takes into account considerable rates of change of curvature. In the present case the value, for either bed or surface, is generally less than 1×10^{-5} day^{-1}.

Comparison of Measured and Theoretical Values of Longitudinal Strain Rate

Table 5-b shows a final comparison between the values of $\dot{\epsilon}_x$. Unfortunately one of the most important terms is invalidated because the

assumptions on which it is based are violated.

At Station 4, however, a calculation of $\dot{\epsilon}_x$ is justified and using surface slopes a value of $+7.7 \times 10^{-5}$ day^{-1} is obtained; using bed slopes a value of 0.5×10^{-5} day^{-1} is obtained. The measured value is seen to lie between these values. Thus, although the computed values of $\dot{\epsilon}_x$ are of the right order of magnitude, agreement is only approximate. Surface stresses have not been computed from the strain rate data but can be found using methods described in Nye (1959b).

Discussion of Previous Comparisons Between Measured and Computed Strain Rates

Table 6 shows a direct comparison between measured and computed values of $\dot{\epsilon}_x$ obtained by Paterson (1962) on Athabaska Glacier, Alberta, Canada, in 1960-61. For complete results of the above investigations see Paterson and Savage (1963a, 1963b) and Savage and Paterson (1963). Paterson uses the expression

$$r = \frac{1}{h}\left(a + \frac{q}{R_s}\cot\alpha\right),$$

which is equivalent to

$$\dot{\epsilon}_x = \frac{a}{h} + \bar{V}_c \kappa_s \cot\alpha ,$$

to compute longitudinal strain rates.

There is no agreement between measured and computed values except at one station*, and this may be fortuitous. Paterson has apparently failed to test whether the curvature term is valid or not in each case. However he attributes this consistent disagreement between observed and theoretical strain rate values to a violation of the assumptions that have been made in deriving the theoretical flow characteristics of ice.

TABLE 6

Comparison of $\dot{\epsilon}_x$ (Calculated) and $\dot{\epsilon}_x$ (Measured) for Athabaska Glacier, Canada. (After Paterson, 1962)

Station	Calculated	Measured
L12	-.105 yr^{-1}	-.068 yr^{-1}
14	.031	-.032
16	.011	-.021
314	-.038	-.020
L19	-.070	-.021
21*	-.024	-.021
23	.023	-.003
25	.029	.002
27	.023	-.001
209	-.022	-.011
L30.5	-.038	-.011
32	.007	-.004
34	.008	-.011

Had Equation (9) been used then certain of the assumptions could have been dispensed with, namely, that ice is a perfectly plastic material, that the shear stress on the bed of the glacier is constant, and that the rate of change of curvature must be small.

Comparison of Laboratory and Field Measurements of Strain Rates

There is generally little agreement between laboratory measurements of the critical strain rate for tensile failure and measurements made on

actual glaciers. The disagreement is generally substantial and may be attributed to

1. The presence of imperfections in glacier ice, such as inclusions and local deformation which would locally change the bulk properties of the ice.

2. The presence of substantial quantitites of firn in the upper zones of glaciers causes a considerable difference in ultimate strength properties from the surface to the base of the tensile layer at which $\sigma_x \leqslant 0$.

3. The development of thermal stresses due to rapid temperature changes at the glacier surface. (Mellor, 1964, p. 85-86)

4. Differences in the rate of mechanical and thermal stress development within the ice.

Discussion of Crevasse Depths

Table 2 shows that computed values of crevasse depth are of the same order as the measured depths which average about 26 meters. Using values of $\dot{\epsilon}$ across a crevasse the average computed depth is about 30 meters, whilst using regional values of strain rate the average computed depths are about 9.5 meters. Moreover, using the value of critical regional strain rate, a tensile layer of 7.5 meters is obtained. Since measured depths, densities, and the flow law constants are considered to be reliable, the problem becomes one of interpreting the strain rate values. To do this, an examination must be made of the methods of obtaining the strain rates and their physical significance.

Two methods were used to obtain $\dot{\epsilon}$ across a crevasse. Several crevasses (3 to 9, Figure 2) were measured for opening rate directly,

so that $\dot{\epsilon} = \frac{\dot{w}_c}{w_c}$; others have been estimated from the regional strain rates using known crevasse spacings and fracture widths. Strain on intercrevasse blocks was assumed to be negligible. Thus d is computed from

$$\frac{1}{\rho g}\left(\frac{\dot{\epsilon}_{crev.}}{B}\right)^{\frac{1}{n}}$$

where $\dot{\epsilon}_{crev.}$ is the strain rate across a crevasse. There is one problem however. It has previously been assumed that $\sigma_{xx} = 0$ across a crevasse and that at the base of an open crevasse $\sigma_{xx} \leq 0$, therefore how is the stress, associated with the strain rate of an air gap, going to be interpreted?

Several methods have been used to compute values of regional strain rates (given in Figure 14-B), and the agreement is within acceptable limits. Values of d less than half of the measured depths are obtain if

$$\frac{1}{\rho g}\left(\frac{\dot{\epsilon}_{xx}}{B}\right)^{\frac{1}{n}}$$

is used. $\dot{\epsilon}_{xx}$ is the regional strain rate.

It will be instructive before proceeding with the discussion to review the results of Meier and others (1957). Meier uses regional strain rates such as those corresponding to $\dot{\epsilon}_{xx}$ and in all cases these are very much smaller than the values used in Table 2 of this report. Strangely, the values of strain rate used by Meier are less than the critical strain rate given elsewhere in his report. It would appear that $\dot{\epsilon}_{xx}$ used in the preceeding equation should be such that $\dot{\epsilon}_{xx} \geqslant \dot{\epsilon}_c$. Furthermore the method that Meier uses to obtain the value of B, in the flow law, is obscure. This empirical constant is extremely temperature sensitive and a change from 0° C to -1.5° C decreases B by an order of magnitude; a change from -1.5° C to -12° C changes its value by a further order of magnitude. Meier's calculations show that if the minimum recorded crevasse

temperature is used to determine B then a depth of 15 meters is obtained (Meier and others 1957, p. 40). Actual temperatures range from -0.5^{o} C to -6.5^{o} C and the mean is probably -3^{o} C, corresponding to a value of B which would give a computed crevasse depth of about 12 meters, which is less than half of the observed depth. Meier assumes a temperature value of -12^{o} C with no apparent justification. However this produces a good correspondence between computed and measured values of d, but since calculations are provided for only two crevasses his results are hardly meaningful.

To return to the problem of the Kaskawulsh Glacier crevasses it must be stated that since crevasses are obviously forming during the summer then values of B and n must be those corresponding to the melting temperature. A depth formula given by $d = 13.5\sigma_x$ is obtained, where σ_x can be determined directly from the curve given by Glen (1953, p. 721), if the value $\dot{\epsilon}_x$ is known. Nye (1955) implies that $\dot{\epsilon}_x$ should be used to compute d, and as mentioned, Meier and others (1957) use values of $\dot{\epsilon}_x$, but clearly, in the present case this is not applicable. Therefore, to solve this dilemma it could be supposed that prior to failure and during crack propagation a local concentration of stress develops. This is associated with a strain rate comparable in magnitude with the values of $\frac{\dot{w}_c}{w_c}$ which have been measured for an opening crevasse. The problem may well be analogous to the case concerning the fracture of metals. Minute surface cracks known as "Griffith cracks" are known to exist in metals before rupture and the local concentrated stress is given by

$$2\sigma_x \left(\frac{l}{R}\right)^{1/2},$$

where $2l$ is the length of the crack, and R is the radius of curvature at the ends of the crack. The average "regional" tensile stress, σ_∞, acts perpendicular to the fracture trace. Clearly, as $R \rightarrow 0$, the local stress may reach very high values. The crack will propagate according to whether this local stress exceeds the ultimate tensile strength of the material.

It is well known that large variations of $\dot{\epsilon}$ occur on the surface of a glacier within short distances (Meier and others, 1957; Nye, 1959b; Paterson, 1962; Wu and Christensen, 1964). Thus the concept of stress concentrations existing on the surface of glacier ice is not unfounded. Finally, it is noted that crevasse depths on temperate glaciers appear to be reasonably consistent.

Discussion of Crevasse Spacing

Crevasse spacing is somewhat of a problem since there is a paucity of analytical work and available data on which to base any hypothesis. As previously stated, it would seem to be necessary to make a stress analysis up glacier of an already formed crevasse. There has been a suggestion that the spacing of crevasses is related to the depth, but this cannot be a simple function since in the present case $s \simeq 2.8\ d$ whereas Meier and others (1957) finds $s \simeq 4\ d$ for certain crevasses on the edge of the ice sheet in northeast Greenland. However, these were not transverse crevasses and the physiographic and thermal environments were much different.

If a simple surface stress distribution is assumed then there is a relation between the spacing of the stress gradient and the critical stress

in tension, but in the present case this relation cannot be tested because the local gradient of strain rate near the uppermost crevasse cannot be accurately obtained. Regional values of this gradient are not appropriate since local values of strain rate commonly vary by an order of magnitude in short distances (see, e.g., Meier and others, 1957; Nye, 1959b; and others).

Using Nielsen's simple bending beam theory a good approximation for the spacing of fractures is obtained. However, assuming S, ρ, and g to be constant in Equation (10), the spacing s should be a function only of the ice thickness h. This conclusion is suspect. Using the data of Meier and others, (1957) for instance, s $\simeq$ 43 meters which is less than half of the measured value of about 4 d $\simeq$ 100 meters. Equation (10), though giving the right order of magnitude of s in the present case, is much too simplified.

There appears to be no reason to associate the spacing of the Kaskawulsh Glacier transverse crevasses with annual movement since the latter is of the order of 110 to 150 $m.yr.^{-1}$. Moreover, the velocity distribution in the area observed has probably a weekly, monthly, or yearly variation of less than ten percent. There is no evidence to suggest that the formation of crevasses is restricted to any part of the year. Crevasses were presumably forming during the summer on Kaskawulsh Glacier. The spacing values, the velocity data, and the flow law at low temperatures suggest that crevasses are forming in the winter also. It may be added, however, that if the velocity of sliding of the glacier is as high at 50% of the total flow velocity, then internal ice velocities range from 55 to 75 $m.yr.^{-1}$, and it is seen that many of the crevasses spacing values lie between 55 and 75 meters (Figure 6).

GENERAL CONCEPT OF TRANSVERSE CREVASE FORMATION

The Kaskawulsh Glacier transverse crevasses appear to be forming under relatively quiet conditions, suggested a more "visco-plastic" behavior of the ice (see Figure 4-B). Crevasse Camp, shown in Figure 2 and Plate 3, was observed at the end of the field season to be situated between two fracture traces, the up glacier one being a firn crack and the lower one being just measurable in width (i.e. by definition, a crevasse) A low altitude flight over the area late in the season revealed the existence of two firn cracks higher up glacier. These cracks are referred to as 01 and 001 (see Figure 2 and Plate 3). Later field measurements of spacing and orientation of these fractures were made but in no case could more than an ill-defined crack be detected. In the remaining two days of the field season these had not opened. To detect their existence by ground visual observation was extremely difficult. Most likely, the fracture at depth was more definite but at the surface firn creep had provided a deep solid bridge which by continuous readjustment removed most of the outward signs of a discontinuity.

To consider the mechanics of formation of these crevasses in previously unfractured firn, it is thought necessary to associate their occurrence with a critical stress and a certain rate of stress development at or near the surface of the glacier. This stress, which is associated with a critical value of extending principal strain rate, is generated by the flow characteristics, dimensions and shape of the ice mass. To a good approximation the crevasse traces form perpendicular to the principal extending strain rate tensor, at a point on the glacier. Presumably the

fracture begins at or near the surface, and propagates to a certain depth given by Equation (5). Further, it is suggested that the initial fracture occurs at or near the ice margins where "shear" crevasses provide a source of weakness in the ice. Later, the crevasse propagates toward the center of the ice stream. The Kaskawulsh Glacier transverse crevasses appear to be forming near the south boundary of the glacier and to be developing quietly toward the central regions. This type of development may not be general however. As the crevasse just formed moves downstream a build-up of surface and subsurface stress behind it takes place until the critical strain rate is again reached, when another fracture is formed. The distance between these two crevasses is probably related to the surface stress gradient or the strain rate gradient. Suggestions have been made that the spacing is closely related to the crevasse depth, but as Meier finds that $s \simeq 4\ d$, and that for the Kaskawulsh Glacier crevasses $s \simeq 2.8\ d$ for comparable depths, the relation cannot be a simple one. In fact a stress analysis around an already opened crevasse needs to be made (Nye, pers. comm.). If the strain rate is effectively zero on an intercrevasse block then the regional strain will be satisfied by the opening, or closing, of the crevasses. However, there is reason to believe that in the present case at least one intercrevasse block had been subjected to sufficient strain so that an intermediate crevasse had formed. This appears to be rather exceptional, however.

Neither detectable vibrations nor the sudden appearance of fractures were ever observed by the occupants of Crevasse Camp, although this was not occupied continuously towards the end of the field season. It is suggested that suitably placed seismograph stations on the glacier could

be used to locate, in time and position, fracture planes in the ice. Suggestions have been made that model studies could be used to elucidate the processes of fracture taking place in glacier ice. Clay models could be, and have been used for qualitative study whilst more quantative experiments could be made using photoelastic techniques.

On real glaciers there is a need for detailed measurements of local strain on the surface and at depth in the region of crevasse origin. Sophisticated methods need to be developed for measuring small strain networks. Further, there is a necessity for obtaining firn and ice samples at depth within the glacier, in order to estimate strength properties of the material.

ACKNOWLEDGEMENTS

This research was conducted as part of The Ohio State University 1964 glaciological program, supervised and led by Dr. C. Bull, on whom the author has been dependent for guidance and valuable consultation.

The Icefield Ranges Research Project, a joint project supported by the Arctic Institute of North America and the American Geographical Society provided all necessary logistics and accommodation during the field season.

Financial assistance was gratefully received from the Bownocker Fund (Department of Geology, Ohio State University), the Friends of Orton Hall Fund (Geology Alumni of The Ohio State University) and the Ohio Academy of Science. Travel expenses and some field equipment were provided by the Institute of Polar Studies of The Ohio State University and the Icefield Ranges Research Program.

I am indebted to members of the staff of the Arctic Institute of North America for their generous cooperation and assistance. The cooperation of the pilot, Mr. Philip Upton, was fully appreciated during the period in the field. In the field, Mr. H. Brecher and Mr. F. Erdmann (Missouri School of Mines) provided valuable and necessary assistance in all phases of the field work.

For being able to use their data the author extends his appreciation to Mr. H. Brecher, Institute of Polar Studies of the Ohio State University; Mr. G. Clarke, of Toronto University; Dr. M. G. Marcus, Department of Geography, University of Michigan; Mr. R. H Ragle, Icefield Ranges Research Project and to Mr. P. Wagner of the University of Michigan.

The Institute of Polar Studies, Ohio State University paid for all drafting. For patient reproduction of most of the figures the author acknowledges the work of Mr. David Gordon of the Institute. Plates 1 and 7 have been kindly provided by Mr. H. Brecher and Mr. F. Erdmann, respectively.

For criticism of the manuscript I am grateful to Mr. H. Brecher, Institute of Polar Studies; Dr. C. Bull, Department of Geology, Dr. R. L. Cameron, Institute of Polar Studies; Dr. R. P. Goldthwait, Department of Geology and Institute of Polar Studies, Dr. J. H. Mercer and Dr. A. Mirsky, Institute of Polar Studies and Dr. H. J. Pincus of the Department of Geology, all at the Ohio State University.

Drs. C. Bull, J. Nye, and J. Weertman provided valuable advice during the preparation of the manuscript.

REFERENCES

Ahlmann, H. W., 1948, Glaciological Research on the North Atlantic Coasts: Roy. Geog. Res. Ser., no. 1, London, 83 p.

Brecher, H. H., 1965, Measurements of short term glacier motion: (unpublished M. Sc. thesis, Department of Geodetic Science, Ohio State University).

Bull, C., and Hardy, J. R., 1956, The determination of the thickness of a glacier from measurements of the value of gravity: Journ. Glac., v. 2, no. 20, p. 755-62.

Butkovich, T. R., 1958, Recommended standards for small scale ice strength tests: U. S. Army SIPRE Tech. Rep. no. 57, 6 p.

----------, and Landauer, J. K., 1959, The flow law for ice: U. S. Army SIPRE Res. Rep. no. 56, 7 p.

Clark, D., 1957, Plane and Geodetic Surveying: v. 1, Ungar Pub. Co., N. Y., 673 p.

Dobrin, M. B., 1960, Introduction to Geophysical Prospecting: 2nd Ed., Mc Graw Hill, N. Y., 446 p.

Glen, J. W., 1952, Experiments on the deformation of ice: Journ. Glac., v. 2, no. 12, p. 111.

---------- , 1953, Rate of flow of polycrystalline ice: Nature, v. 172, p. 721-22.

---------- , 1955, The creep of polycrystalline ice: Proc. Roy. Soc., Ser. A, v. 228, p. 519-38.

---------- , 1963, The rheology of ice: in Kingery, W. D., 1963, Ice and snow: The M. I. T. Press, Cambridge, Mass., p. 3-7.

Gold, L. W., 1960, The cracking activity in ice during creep: Can. Journ. Phys., v. 38, no. 9, p. 1131-1148.

Goldthwait, R. P., 1936, Seismic sounding on South Crillon and Klooch Glaciers: Geog. Journ., v. LXXXVII, no. 6, p. 503.

Hauser, F. E., Landon, P. R., and Dorn, J. E., 1956, Deformation and fracture mechanisms of polycrystalline magnesium at low temperatures: Trans. Am. Soc. Metals, v. 48, p. 986-1002.

Hill, R., 1950, The mathematical theory of plasticity: Oxford, Clarendon Press, 356 p.

Hobbs, W. H., 1911, Characteristics of existing glaciers: Macmillan Co., N. Y., 301 p.

Kamb, B., and La Chapelle, E., 1964, Direct observation of the mechanism of glacier sliding over bedrock: Journ. Glac., v. 5, no. 38, p. 159.

Kanasewich, E. R., 1963, Gravity measurements on the Athabaska Glacier, Alberta, Canada: Journ. Glac., v. 4, no. 35, p. 617-32.

Lagally, M., 1929, An attempt to formulate a theory of crack formation in glaciers: U. S. Army SIPRE Transl. no. 47.

Lewis, W. V., 1949, Glacier movement by rotational slipping: Geograf. Ann. band XXI, no. 1, p. 146.

Lliboutry, L., 1958, Glacier mechanics in the perfectly plastic theory: Journ. Glac., v. 3, no. 23, p. 167.

Loewe, F., 1955, The depth of crevasses: Journ. Glac., v. 2, no. 17, p. 511-12.

Marcus, M. G., 1965, Summer temperature relations in the St. Elias Mts, Alaska and Yukon Territory: University of Colorado Studies, 1965, (in press).

Meier, M. F., and others, 1957, Preliminary study of crevasse formation: U. S. Army SIPRE Rep. no. 38, 80 p.

---------- , 1960, Mode of flow of Saskatchewan Glacier, Alberta, Canada: U. S. G. S. Prof. Paper 351, 70 p.

Mellor, M., 1964, Snow and ice on the earths surface: U. S. Army CRREL Cold Regions Sci. and Eng., Pt II, Sec. C, p. 65-89.

Meyerhof, G. G., 1964, Crevasse depths: in The mechanics of glacier flow (Discussion): Journ. Glac., v. 2, no. 15, p. 340.

Nielsen, L. E., 1955, Regimen and flow of ice in equilibrium glaciers: Bull. Geol. Soc. Am., v. 66, no. 1, p. 1-8.

----------, 1958, Crevasse patterns in glaciers: American Alpine Journ., N. Y., p. 47.

Nye, J. F., 1951, The flow of glaciers and ice sheets as a problem in plasticity: Proc. Roy. Soc., Ser. A, v. 207, p. 554-72.

--------- , 1952, The mechanics of glacier flow: Journ. Glac., v. 2, no. 12, p. 82-93.

--------- , and others, 1954, The mechanics of glacier flow (Discussion): Journ. Glac., v. 2, no. 15, p. 339-341.

Nye, J. F., 1955, Correspondence on crevasses: Journ. Glac., v. 2, no. 17, p. 512-14.

----------, 1957a, The physical properties of crystals: Oxford, Cambridge, p. 158-63.

--------- , 1957b, Glacier mechanics: Journ. Glac., v. 3, no. 22, p. 91-3.

--------- , 1957c, The distribution of stress and velocity in glaciers and ice sheets: Proc. Roy. Soc., Ser. A, v. 239, p. 113-33.

--------- , 1959a, The deformation of a glacier below an ice-fall: Journ. Glac., v. 3, no. 25, p. 387.

--------- , 1959b, A method of determining the strain rate tensor at the surface of a glacier: Journ. Glac., v. 3, no. 25, p. 409-18.

--------- , 1959c, The motion of ice sheets and glaciers: Journ. Glac., v. 3, no. 26, p. 493-507.

--------- , 1960, The response of glaciers and ice sheets to seasonal and climatic changes: Proc. Roy. Soc., Ser. A, v. 256, no. 1287, p. 559-84.

--------- , 1963, The response of a glacier to changes in the rate of nourishment and wastage: Proc. Roy. Soc., Ser. A, v. 275, p. 87-112.

Orowan, E., 1964, Continental drift and the origin of mountains: Science, v. 146, no. 3647, p. 1003-10.

Paterson, W. S. B., 1962, Observations on Athabaska Glacier and their relation to the theory of glacier flow: (Ph. D. thesis, University of British Columbia, Canada).

---------- , and Savage, J. C., 1963a, Geometry and movement of Athabaska Glacier: Journ. Geophys. Res., v. 68, no. 15, p. 4513-20.

---------- , and Savage, J. C., 1963b, Measurements on Athabaska Glacier relating to the flow law of ice: Journ. Geophys. Res., v. 68, no. 15, p. 4537-43.

---------- , 1964, Variations in velocity of Athabaska Glacier with time: Journ. Glac., v. 5, no. 39, p. 277.

Prandtl, L., 1923, Z. Angew. Math. Mech: v. 3, p. 401.

Rigsby, G. P., 1958, Effect of hydrostatic pressure on velocity of shear deformation of single ice crystals: Journ. Glac., vv. 3, no. 24, p. 273.

Russel, R. D., and others, 1960, Gravity measurements on Salmon Glacier and adjoining snow fields, British Columbia, Canada: Bull. Geol. Soc. Am., v. 71, no. 8, p. 1223-29.

Savage, J. C., and Paterson, W. S. B., 1963, Borehole measurements on the Athabaska Glacier: Journ. Geophys. Res., v. 68, no. 15, p. 4521-36.

Schuster, R. L., 1954, Travel and rescue in crevassed areas: U. S. Army SIPRE Instruction manual no. 2, 10 p.

Schuster, R. L., and Rigsby, G. P., 1954, Preliminary report on crevasses: U. S. Army SIPRE Spec. Rep. no. 11.

Sharni, D., 1963, Icefield Ranges Research Project: Survey Report, Institute of Polar Studies, Ohio State University.

Seligman, G., 1955, Comments on crevasse depths: Journ. Glac., v. 21, no. 17, p. 514.

S. I. P. R. E. Report 4, 1951, Review of the properties of snow and ice: University of Minnesota, Inst. Techn. Eng. Exp. Sta., U. S. Army SIPRE contract. Many authors. 156 p.

Steinemann, S., 1958, Experimentelle Untersuchungen zur Plastizität von Eis: Beit. Geologie der Schweiz. Hydrologie, no. 10, p. 50.

Taylor, L. D., 1962, Ice structures, Burroughs Glacier, Southeast Alaska: (Ph D. dissertation, Department of Geology, Ohio State University).

Theil, E., and others, 1957, The thickness of Lemon Creek Glacier, Alaska, as determined by gravity measurements: Trans. Am. Geophys. Union, v. 38, no. 5, p. 745-49.

Wagner, P., 1963, Snow facies studies on the Kaskawulsh Glacier, Yukon Territory, Canada: (M. Sc. thesis, University of Michigan).

--------- , 1964, Diagenesis and snow facies: I. R. R. P. 1962-63: Arctic, v. 17, no. 1, p. 56.

Weertman, J., 1957, On the sliding of glaciers: Journ. Glac., v. 3, no. 21, p. 33.

---------- , 1964, The theory of glacier sliding: Journ. Glac., v. 5, no. 39, p. 287.

Wheeler, J. O., 1963, Geology of Kaskawulsh, Mt. St. Elias, east half, Yukon Territory, Canada. (Map) 1 inch to 4 miles, no. 1134A Geol. Surv. Can., Department of Mines and Technical Surveys.

Wood, W. A., 1963, The Icefield Ranges Research Project: Geog. Rvw., v. LIII, no. 2, p. 163-84.

Wu, T. N., and Christensen, R. W., 1964, Measurements of surface strain rate on Taku Glacier, Alaska: Journ. Glac., v. 5, no. 39, p. 305 -313.

APPENDIX I

NOTES ON THE MORPHOLOGY AND STRATIGRAPHY OF CREVASSES

An initial fracture plane is for practical purposes perpendicular to the glacier surface, so that in the present case the cracks are essentially vertical. Further, since the depth of crevasses here is only four percent of the total ice thickness, little distortion of the crevasse plane is expected due to vertical changes in longitudinal velocity and strain rate. Measurements show that these crevasses are opening as "rigid wedges", or, if a compressive flow field is entered, closing as "rigid wedges". The latter term is probably only appropriate for cases in which the ice is subjected to bending. Small deviations in crevasse wall angle can be explained by appealing to secondary deposition and inhomogeneity of the properties of the ice being ruptured. Observed crevasses varied in width from zero to five meters or more, while the average depth was about 26 meters. Water existed in the bottoms of most crevasses examined later in the ablation season; the conclusions drawn from this have been mentioned elsewhere.

Snow-bridges were examined and are discussed next. They are of particular importance to the polar and alpine researcher and to the alpinist. Two bridge sections were examined in some detail (Figure 18). General observations indicate that:

1. Laterally, bridge thicknesses vary greatly. Within several tens of meters a bridge could be almost breached whereas elsewhere it may be 2 meters thick, sufficient to withstand the passage of a motor toboggan or a skier.

2. Bridges are initially formed by aeolian agencies; cornices form from material stripped from the snow surface. Development of cornices can be highly variable locally. Dominant winds are north-east and south-west, favourable to rapid bridge development. In most cases later deposits appear to be the result of normal direct accumulation.

3. The center of the lower side of the bridge possesses a steep triangular cleft which is the result of opening of the crevasse and bending of the bridge. Icicles and hoar crystals are common on the base of bridges and on wall ice growths (Plates 7 and 8). Icicles possess an unusual crystallographic orientation, the reason for which is not known (Hoerni, in Meier and others, 1957). Since icicles are up to a meter long, body forces may be sufficient to cause some alignment of the c-axes.

4. Bridges over narrow crevasses are thinner than those over wide crevasses. Early in the season many of the crevasses were so effectively bridged that detection was possible only under certain lighting conditions. Later in the summer ablation had thinned the bridges and strain had weakened them so that distinct sags developed. Sags are a function of bridge width. Remanent bridges were often found wedged between the crevasse walls at some depth.

Figure 19 shows a typical stratigraphic section on the wall of a crevasse. Detailed interpretation of stratigraphy is beyond the scope of this thesis. Excess percolation and "soaking" of successive layers renders any interpretation extremely difficult. Geochemical methods are invalidated here. The approximate density profile enables an estimate to be made of the mean density from $\rho_m = \frac{\int_0^d \rho_z \, dz}{d}$. Annual accumulation is high (Table 1). During the summer the snow pack is classified as

belonging to the saturation zone and within two years the snow has reached the status of firn.

The 0^{o} C isotherm was recorded from the surface to 24 meters late in the season. Free water existed in the bottoms of most crevasses during August. These and other data suggest that this part of the glacier is geophysically temperate.

Thick layers of blue and white ice (up to 30 centimeters) should be studied crystallographically in order to determine the effects of rupturing.

APPENDIX II

METEOROLOGICAL DATA

Summary of Meteorological Data for Divide Station, St. Elias Mountains, Yukon Territory, Canada. (after Marcus, 1965)

Location: Lat. 60°47'N., Long. 139°40'W. Elev. 2640 m.
Period of observations: 1 July to 17 August, 1964.

Date	Precip. cm. snow	Air. Temp. (°F) Max.	Min.	Wind Vel. mph.	Wind Dir.	Rel. Hum. (%)	Duration Sun (hr.)	Cloud 10/10	Cond. of crev.
1 Jul	0.1	26.0	18.2	11	SE	85.8	3.3	9.1	Well
2	1.6	27.0	19.3	11	SE	91.8	1.2	8.4	brid-
3	0.1	26.7	20.1	10	SE	91.9	0.8	9.0	ged.
4	0.3	27.0	10.0	4	SE	89.0	8.7	7.5	
5		31.3	9.8	1	SW	88.1	5.5	7.6	
6	T	34.0	5.8	3	NE		12.1	4.0	
7	2.0	32.0	24.0	9	N	87.6	1.9	9.4	
8	0.6	32.0	21.3	9	SE	89.8	7.5	7.1	
9	3.8	33.0	19.3	6	E	83.9	5.6	6.8	
10	1.5	26.0	19.7	12	SW	95.1	0.0	9.8	
11	T	27.3	19.1	7	SE	90.9	1.8	9.1	
12	1.0	20.0	20.2	3	SW	91.8	6.5	7.3	
13	T	44.0	22.9	5	N	88.6	10.5	5.1	
14		47.8	22.3	1	SE	77.3	16.5	1.1	
15		46.1	19.2	1	N	63.5	16.5	1.3	
16		39.9	17.3	1	W	58.4	15.1	0.8	
17		41.0	21.0	2	SW	71.9	16.5	0.9	
18		51.3	20.9	1	SE	67.6	16.1	2.5	
19		44.0	21.8	1	SE		11.2	4.6	
20		35.5	21.8	3	NE		12.4	5.8	
21		39.6	17.8	2	S	90.4	13.1	0.9	
22	0.8	32.0	20.3	6	SW	93.6	1.7	8.9	
23	0.8	28.3	20.5	8	E	92.3	2.2	9.6	
24		28.2	20.3	8	SW	94.1	0.2	10.0	
25	6.4	26.3	17.8	2	NE		0.9	9.0	
26	T	34.0	22.5	8	NE	88.8	10.6	4.8	
27	0.2	29.9	27.6	15	NE		0.0	10.0	Thin-
28		34.0	25.0	6	E		3.9	9.1	ning
29		42.0	26.9	3	SW		11.0	6.1	of
30		35.0	24.5	6	NE		3.2	8.0	brid-
31	8.4	33.0	30.0	8	E		0.1	10.0	ges.

Appendix II (continued)

Date	Precip. cm. snow	Air Temp. (°F) Max.	Min.	Wind Vel. mph.	Wind Dir.	Rel. Hum. (%)	Duration Sun (hr.)	Cloud 10/10	Cond. of crev.
1 Aug	3.2	43.0	29.6	2	NE		1.6	10.0	De-
2	T	34.4	28.8	4	E		7.0	7.9	cay
3	T	40.0	21.5	1	NE		3.6	6.6	of
4	T	31.0	12.0	5	SW		2.5	9.0	brid-
5		34.0	13.0	3	SW		7.1	6.4	ges.
6	T	32.0	17.0	3	E		4.0	6.8	
7		42.0	18.7	3	NE		5.2	6.0	
8	T	43.0	17.6	2	E		11.1	3.1	Water
9	0.4	31.2	12.2	6	SE		4.5	9.1	in
10	2.1	32.3	22.4	7	NE		2.2	9.3	all
11	0.6	36.3	26.0	8	NE		7.0	7.0	crev.
12	3.1	31.6	20.2	10	SE		3.4	7.8	obsv.
13	T	30.8	18.8	6	E		6.1	7.5	
14		30.3	14.2	3	NE		10.1	4.3	
15	0.5	30.0	15.3	4	NE		9.1	5.0	
16	0.2	40.0	14.8	1	NE		11.7	7.1	

APPENDIX III

COMPUTATION OF SURFACE STRESSES

Nye (1959b, p. 414) outlines a method of computing stresses from the measured surface strain rates by using the experimental results of Glen (1955). The flow law relation, which is of the quasi-viscous type, is not the same as that used in the computation of crevasse depths made in the section on Field Data and Results. The reason for this is due to further research into the flow behavior of ice subjected to low stresses. A re-calculation of crevasse depths, using the results of more recent flow law investigations, will be made in Appendix IV. The stress-strain relation used in the present computations is of the form $\dot{e} = 0.148\,\tau^{4.2}$.

The following table shows the principal stresses at Stations 1, 2 and 3.

Diamond #	$\dot{\epsilon}_1$	$\dot{\epsilon}_2$	$\dot{\epsilon}_3$	$\dot{e}$ (yr^{-1})	τ (bars)
3	$+4.35 \times 10^{-5}$ day^{-1} ($0.01596\ yr^{-1}$)	-9.10×10^{-5} day^{-1} ($0.03324\ yr^{-1}$)	($+0.01728\ yr^{-1}$)	0.0287	0.677
2	$+10.24 \times 10^{-5}$ day^{-1} ($0.0374\ yr^{-1}$)	-10.26×10^{-5} day^{-1} ($0.03743\ yr^{-1}$)	($+0.0006\ yr^{-1}$)	0.0374	0.721
1	$+14.35 \times 10^{-5}$ day^{-1} ($0.0525\ yr^{-1}$)	-14.0×10^{-5} day^{-1} ($0.0511\ yr^{-1}$)	($-0.0014\ yr^{-1}$)	0.0519	0.781

	σ_1'	σ_2'	σ_3'	σ_1	σ_2	GRID BEARING OF: $\dot{\epsilon}_1$	Velocity Vector
3	+0.376	-0.785	+0.408	+0.033	-1.194	79.4°	71.0°
2	+0.722	-0.723	+0.012	+0.721	-0.724	89.1°	74.5°
1	+0.790	-0.769	-	+0.811	-0.748	87.5°	72.5°

Appendix III (continued)

Since the relation $\dot{\epsilon}_1 + \dot{\epsilon}_2 + \dot{\epsilon}_3 = 0$ holds for a constant volume condition, the presence of crevasses within most of the diamonds may cause appreciable errors in $\dot{e}$ and hence $\frac{\tau}{\dot{e}}$, σ_t', σ_1 and σ_2. The last two columns of the above table indicate that there is a substantial but consistent difference of between 8^o and 15^o between the principal extending strain rate direction and the direction of the total velocity vector. Nye (1959b, p. 415) shows differences of between 5^o and 22^o but these are not consistent with regard to algebraic sign. Estimates from the data of Wu and Christensen (1964) suggest differences of the order 8^o to 30^o. These are consistent in that principal extending strain rate directions are clock-wise of the total velocity vectors. This is exactly the case for the present results. Some significance may be attached to these results.

APPENDIX IV

COMPARISON OF THEORETICAL CREVASSE DEPTHS USING TWO FLOW LAWS FOR ICE

Computations, which are summarized in Table 2, p. 42, show that in order to obtain a better correspondence between theoretical and observed crevasse depths, the strain rate across a crevasse must be used. The flow law employed is $\dot{\epsilon} = 0.17\sigma^{3.17}$ which applies at -0.02° C (Glen, 1955, p. 528). This yields an expression (5)

$$d = \frac{1}{\rho g}\left(\frac{\dot{\epsilon}}{0.17}\right)^{0.3155}$$

which reduces to

$$24.90\,(\dot{\epsilon})^{0.3155}$$

If a creep rate of $0.017\sigma^{4.2}$ is used (Glen, 1955, p. 530), then an approximate depth formula $d = 37.5\,(\dot{\epsilon})^{0.238}$ is obtained. This clearly gives higher values of depth than the former expression. The table below summarizes certain values of depths of the tensile zone using various formulae and strain rates.

Crevasse #	Strain Rates		Depths (m)				
	across crev. yr^{-1}	regional, yr^{-1}	$24.90(\dot{\epsilon})^{0.3155}$		$37.5\,(\dot{\epsilon})^{0.238}$		measured
			crev.	reg.	crev.	reg.	
7	1.5	0.022	29.8	8.2	41.3	15.1	26
10	1.3	0.037	27.0	9.7	39.8	17.1	27
14	0.8	0.046	24.5	10.1	35.5	18.4	26.5

Clearly, with but few exceptions, the same order of magnitude of values of d are obtained; regardless of the exactness of the flow law expression it becomes apparent that the critical parameter is the value of the strain rate. The main deduction here is that observed crevasse depths do not vary as greatly as the theoretical equations suggest. Further, the appropriate strain rate for computing crevasse depths is close to the localized crevasse strain rates. It should be noted that the assumption is made that the flow law derived by Glen is valid for surficial glacier ice, which has been fractured.

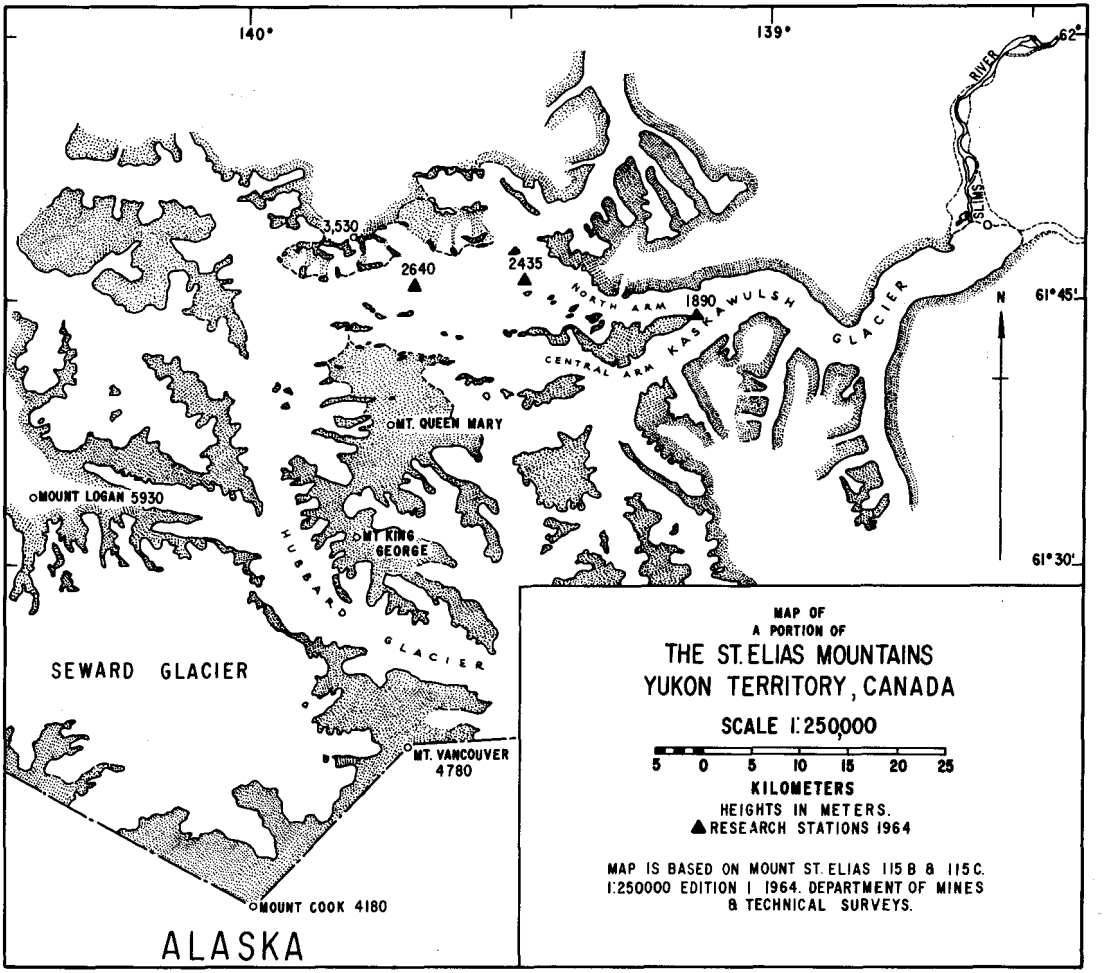

Figure 1. Locality map. Crevasse Camp (2435 m.) is at latitude 61°46'N., longitude 139°30'W. Divide Camp (2640 m.) is at latitude 61°46'N., longitude 139°40'W.

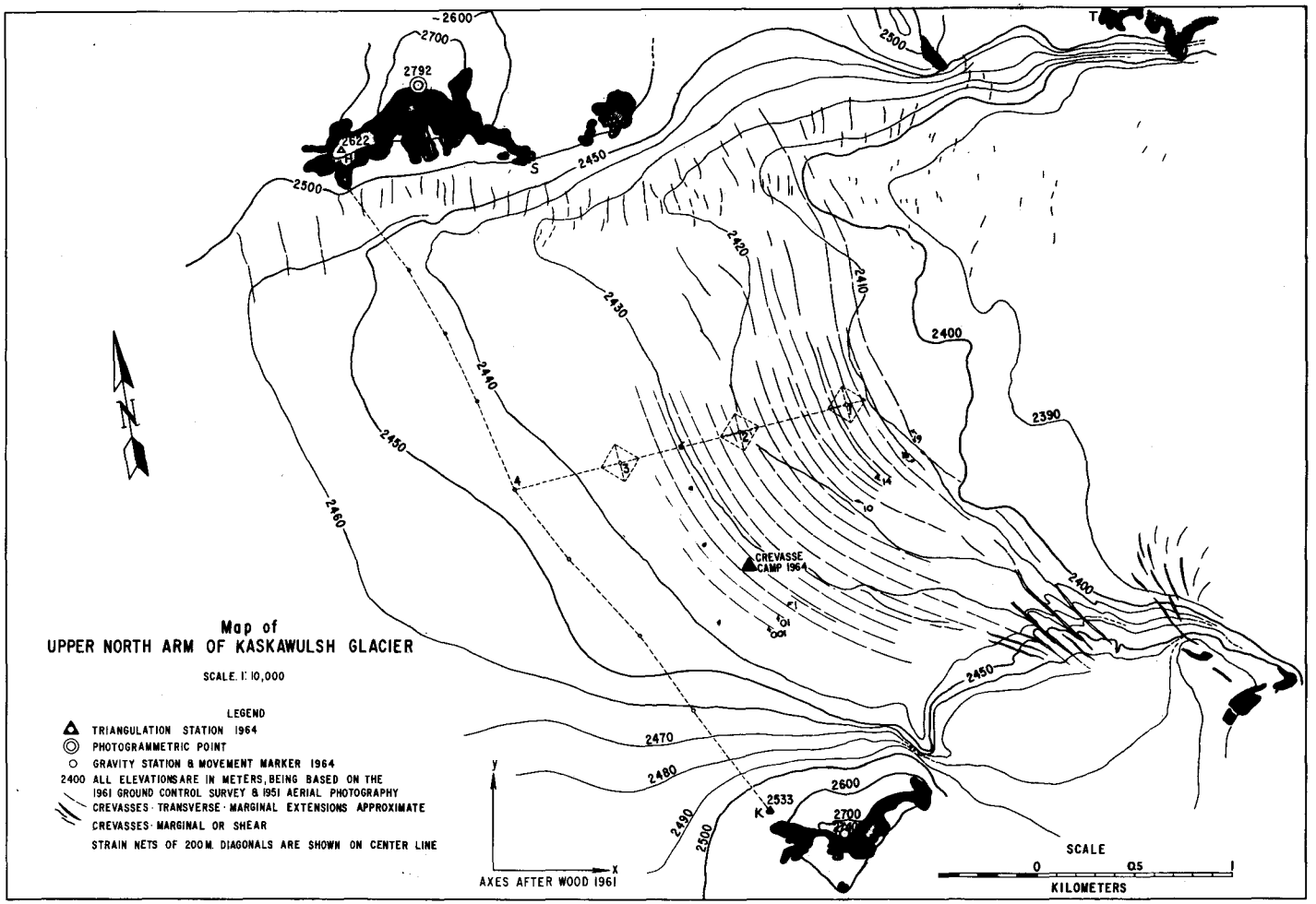

Figure 2. Geometry of the survey network and the configuration of the transverse crevasse field.

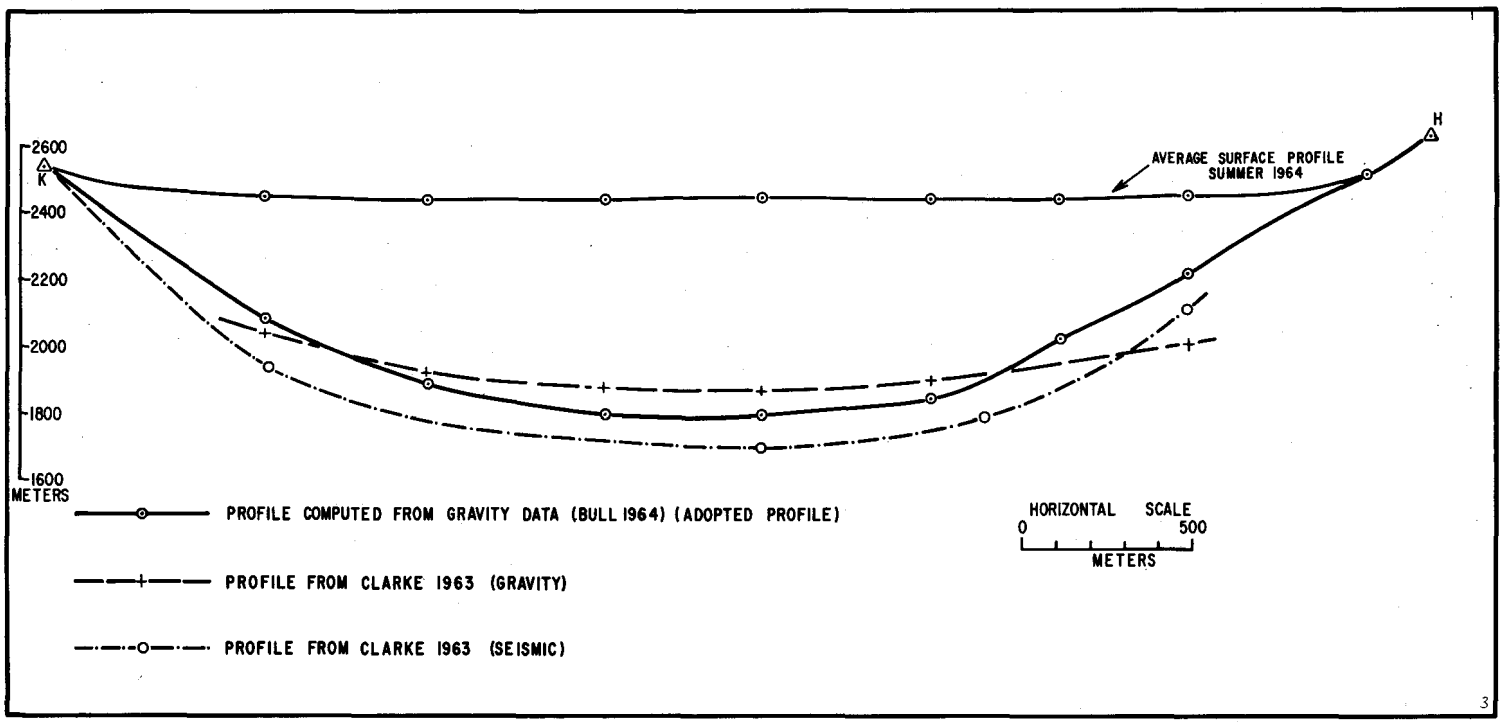

Figure 3. Computed cross-sections of Kaskawulsh Glacier between stations H and K.

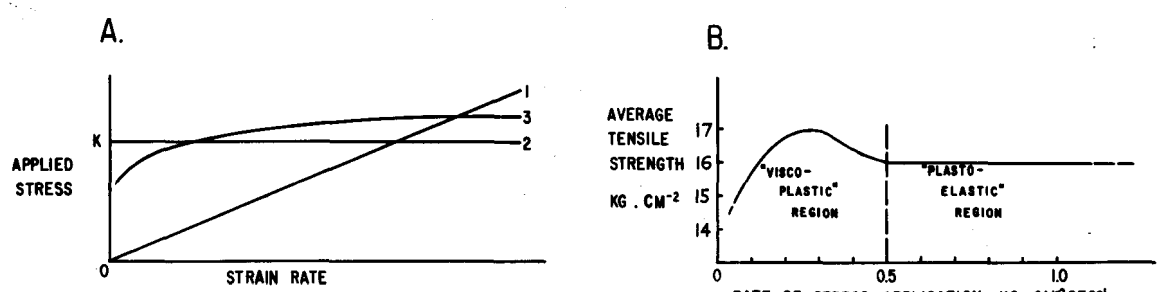

Figure 4. Generalized relations between (A) applied stress and strain rate: 1, Newtonian liquid; 2, perfectly plastic solid. K is the yield stress; 3, ice (after Glen, 1952); and (B) ultimate tensile strength and rate of loading of ice (after Butkovich, 1958).

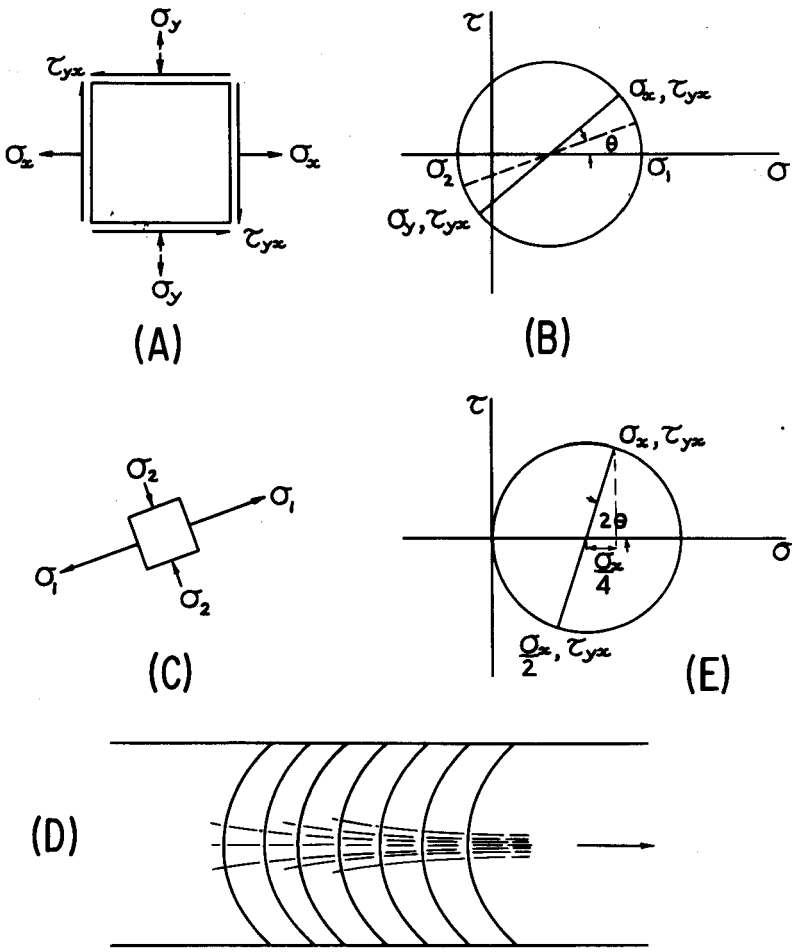

Figure 5. (A) Stress block for element of ice subjected to extending flow. (B) Mohr's circle construction for finding principal stresses. (C) Principal axes of stress. (D) Typical crevasse patterns. Transverse fractures are associated with $\sigma_1 > 0 > \sigma_2$. Longitudinal fractures are associated with $\sigma_2 > 0$, $\tau_{xy} \leq \left|\frac{\sigma_x}{\sqrt{2}}\right|$. Ice flows to right. (E) Limiting case where $\sigma_2 \geq 0$.

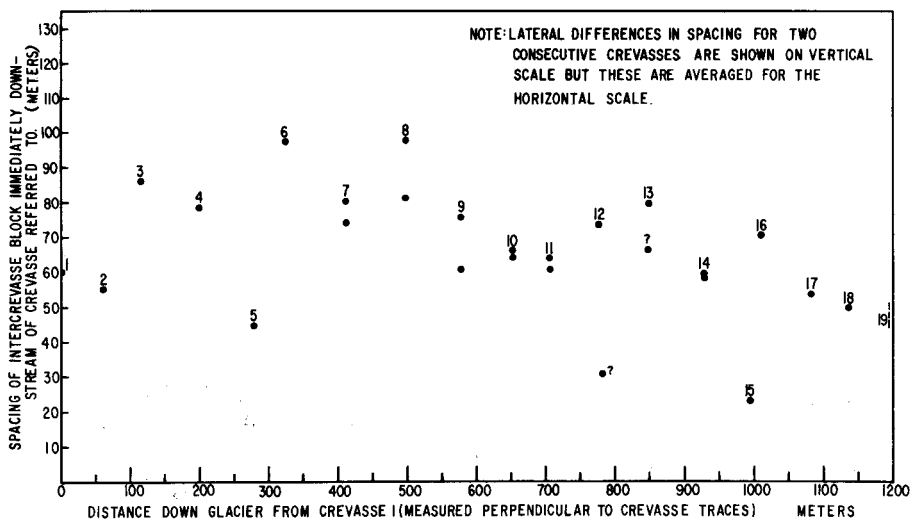

Figure 6. Plot of crevasse spacing with distance down glacier.

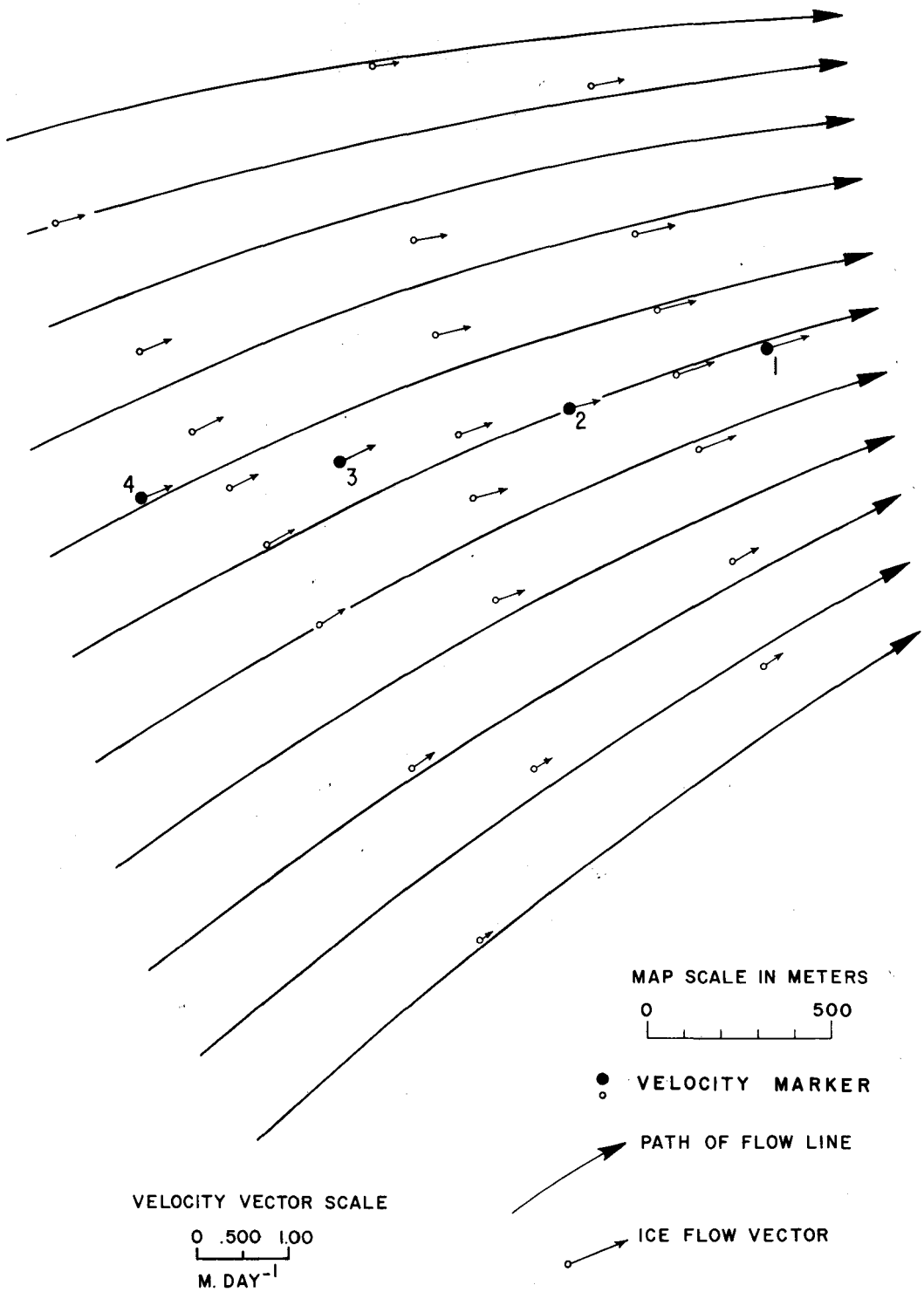

Figure 7. Configuration of flow-line field based on velocity data.

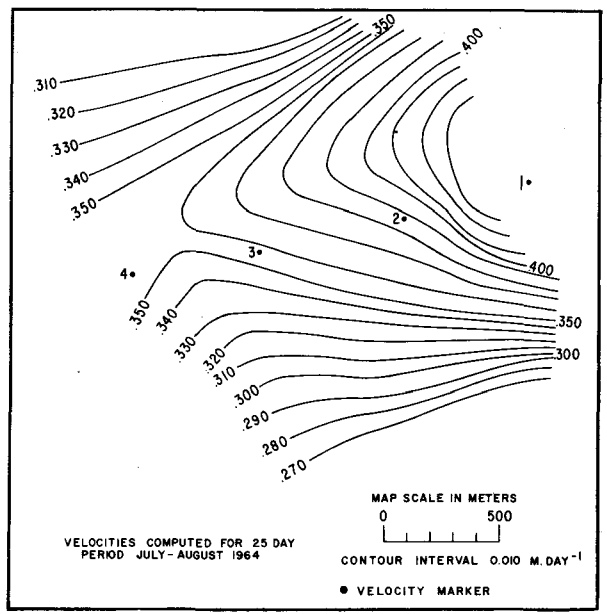

Figure 8. Contours of total velocity V, m. day^{-1}.

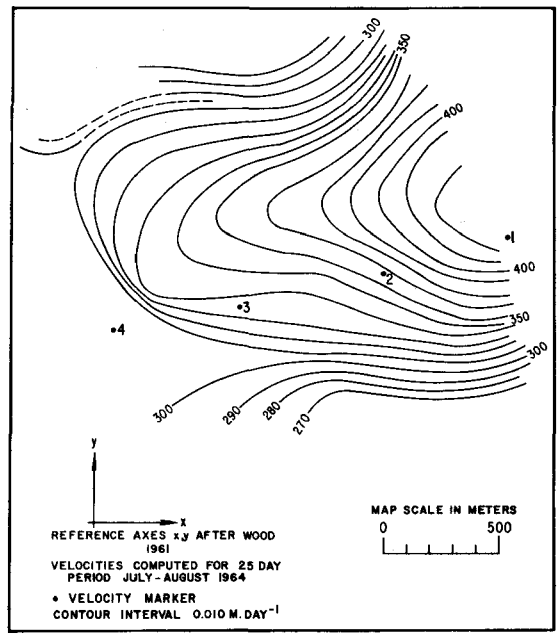

Figure 9. Contours of velocity component V_X, m. day^{-1}.

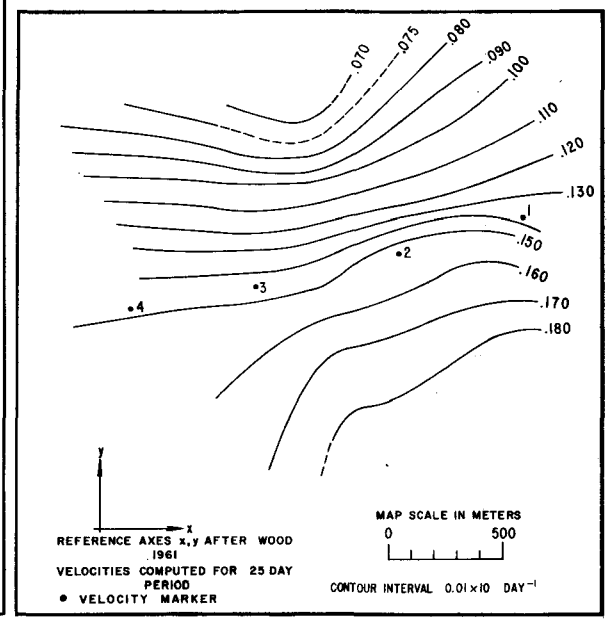

Figure 10. Contours of velocity component V_Y, m. day^{-1}.

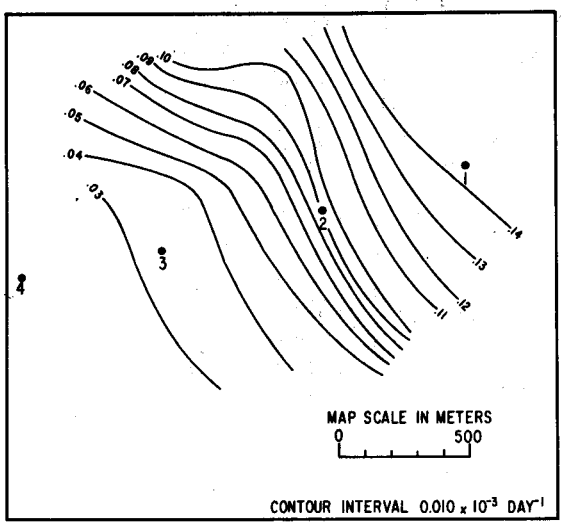

Figure 11. Contours of principal extending strain rate ($\dot{\epsilon}_1$).

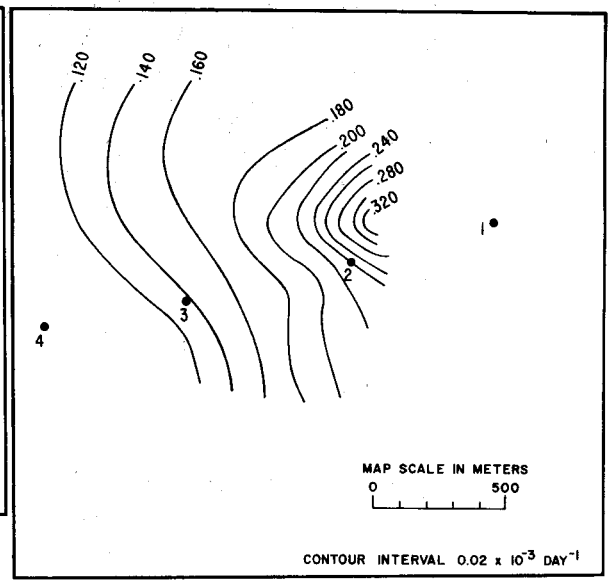

Figure 12. Contours of principal contracting (least extending) strain rate ($\dot{\epsilon}_2$).

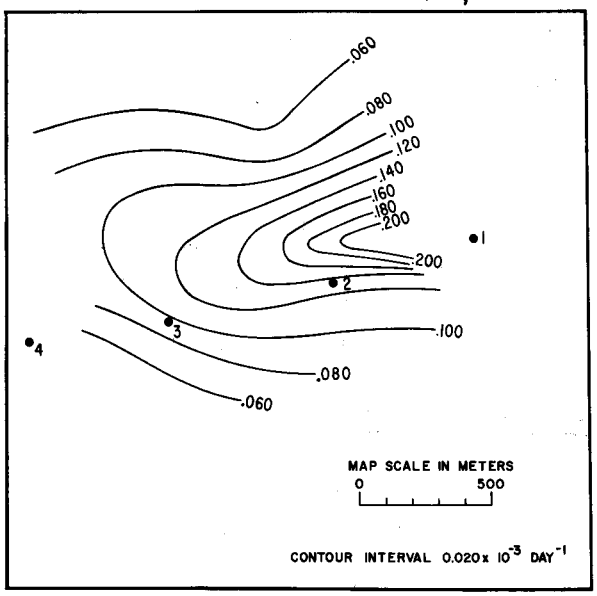

Figure 13. Contours of maximum shearing strain rate ($|\dot{\epsilon}_1 - \dot{\epsilon}_2|$).

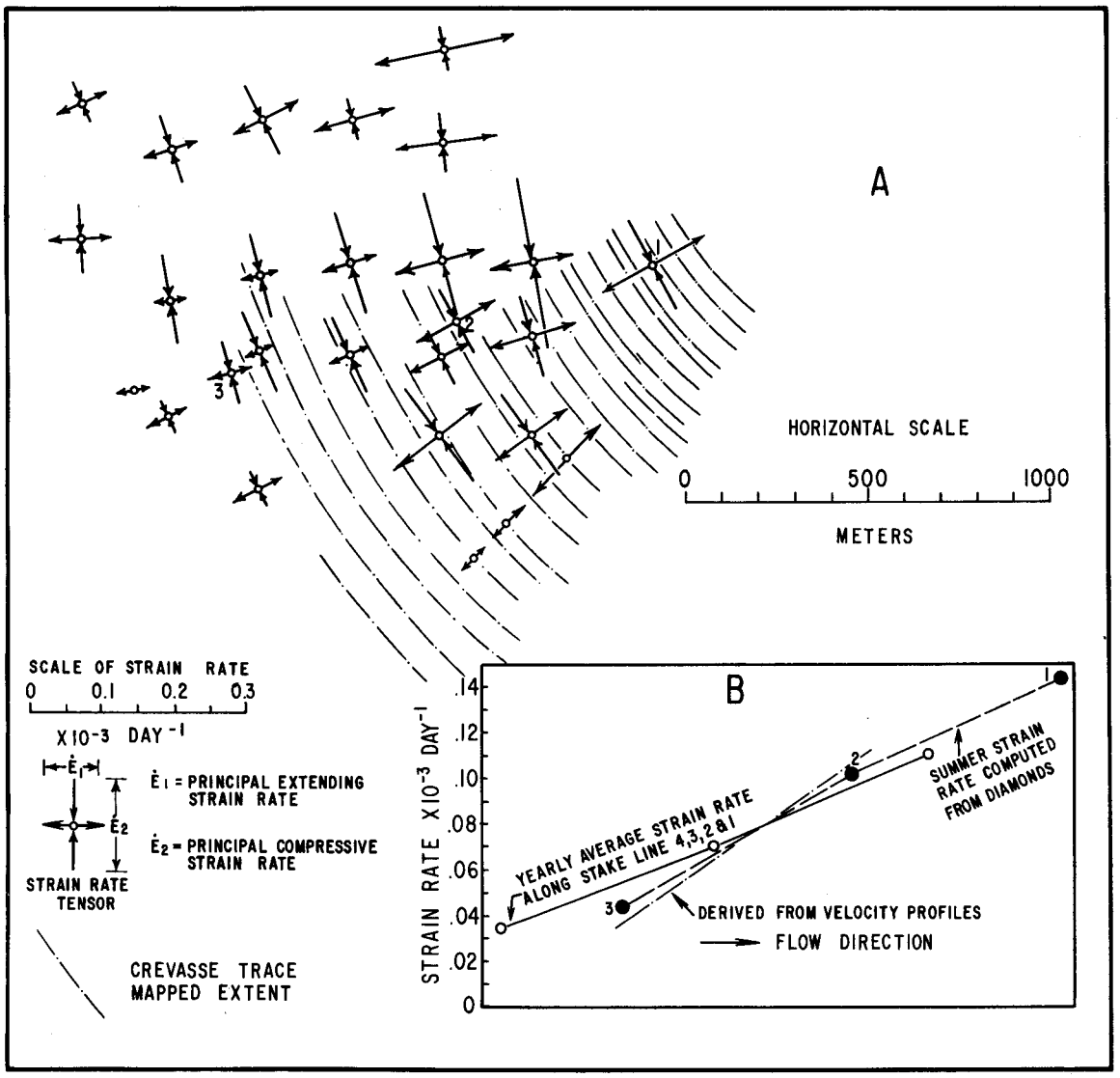

Figure 14. (A) Configuration of principal strain rate field in region of the transverse crevasses. (B) Longitudinal variation of principal extending strain rate.

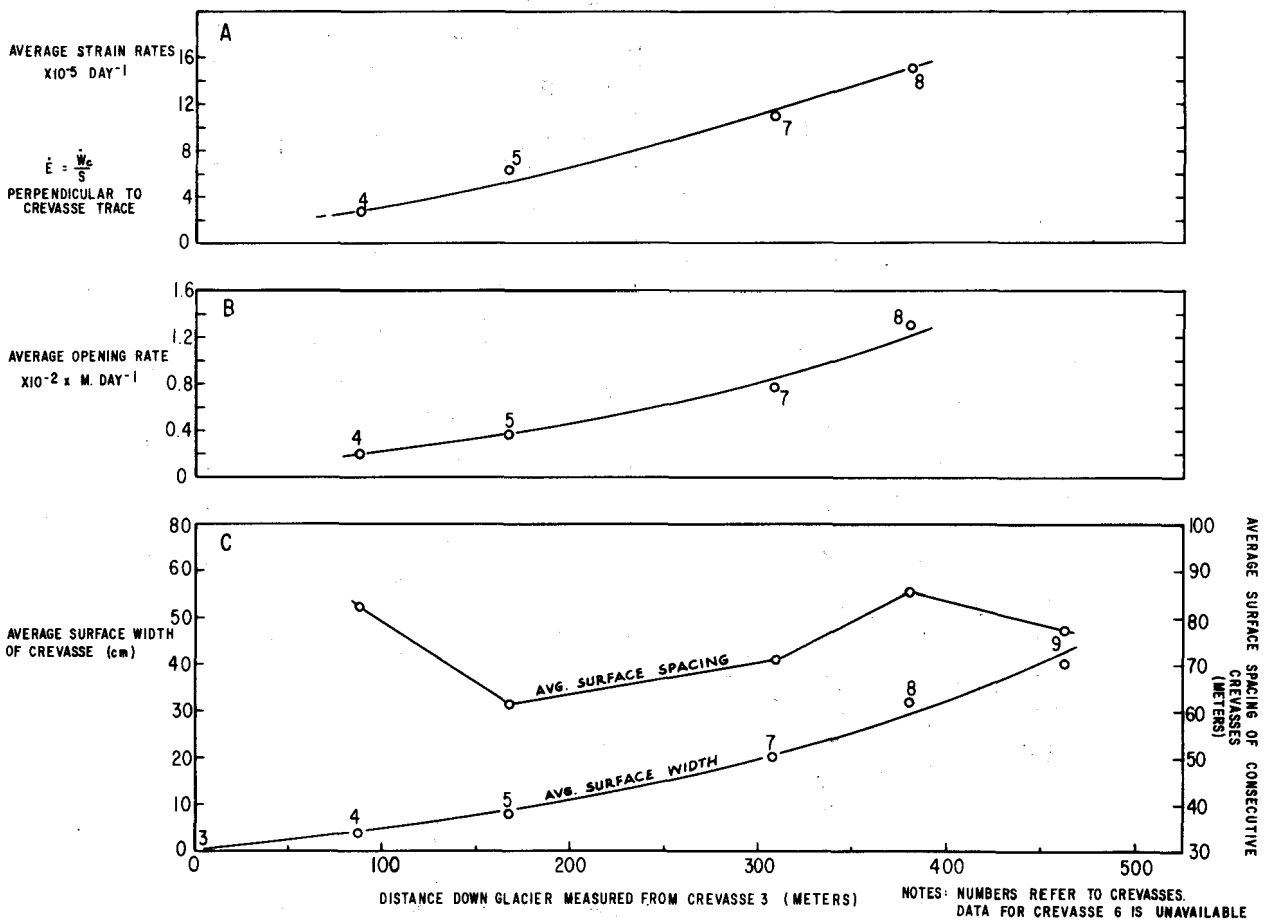

Figure 15. (A) Approximate extending strain rate gradient perpendicular to crevasse traces ($\dot{\epsilon} = \frac{\dot{W}c}{S}$). (B) Variation of crevasse opening rate ($\dot{w}c$) down glacier. (C) Surface width (ω_c) and spacing (S) of crevasses 3 to 9.

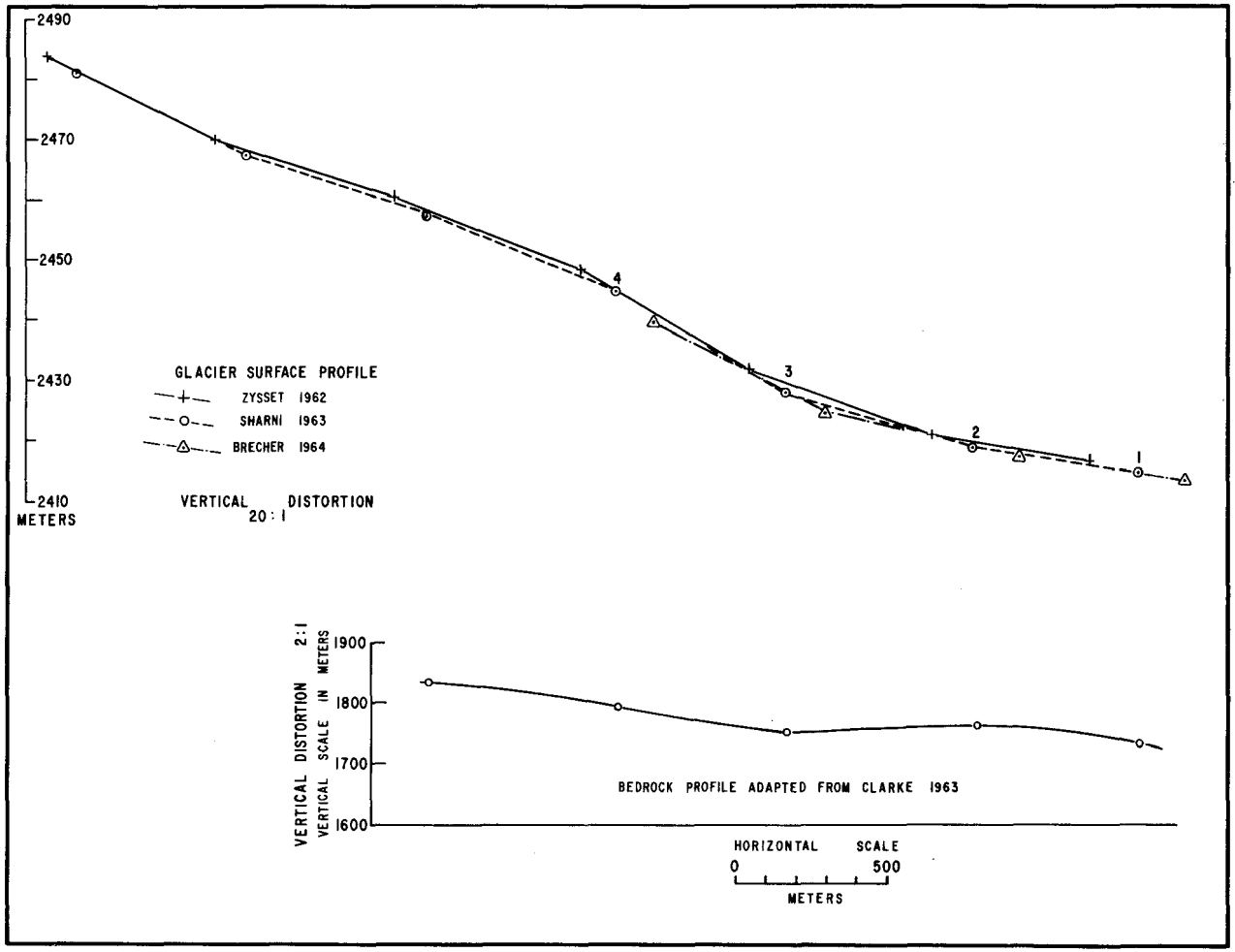

Figure 16. Longitudinal profile of glacier surface and bedrock along central markers 1 through 4 (located in figure 2). Sources of data are given.

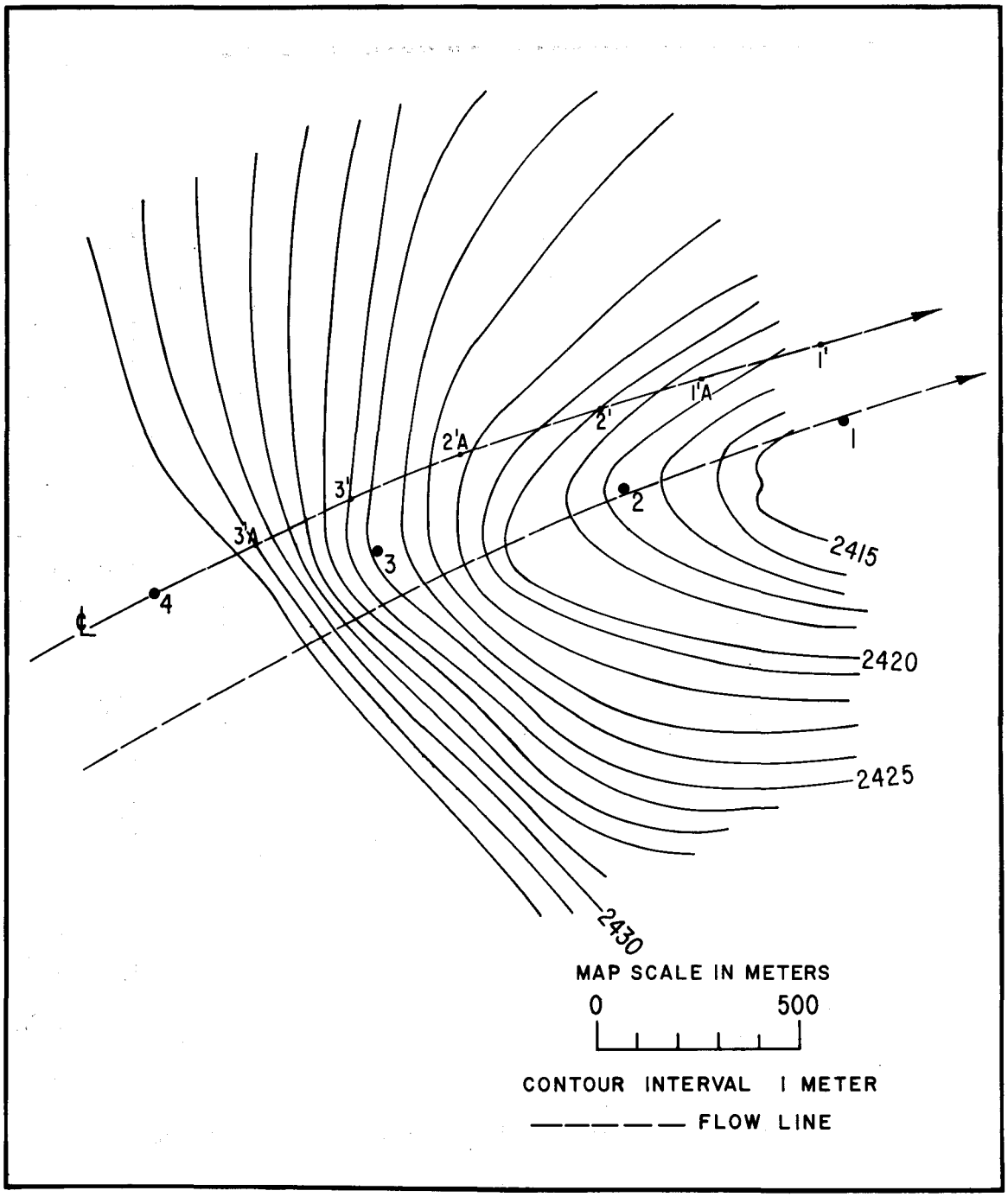

Figure 17. Average surface configuration, July 1964. Flow-line through marker 4 is the "dynamic" center-line; flow-line through 1 and 2 is the "geographic" center-line.

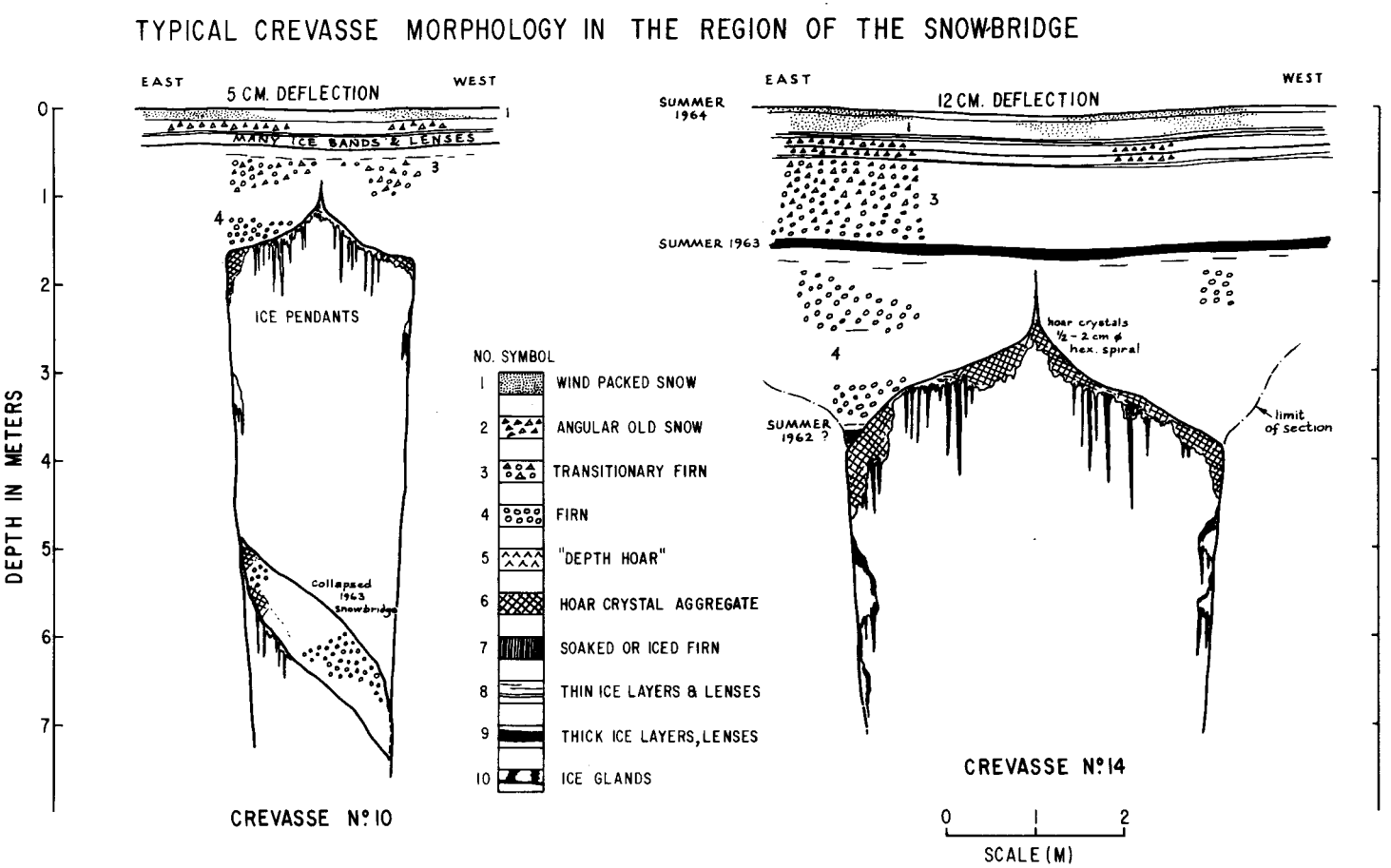

Figure 18. Sections across crevasses no. 10 and no. 14 in the region of the snow-bridge.

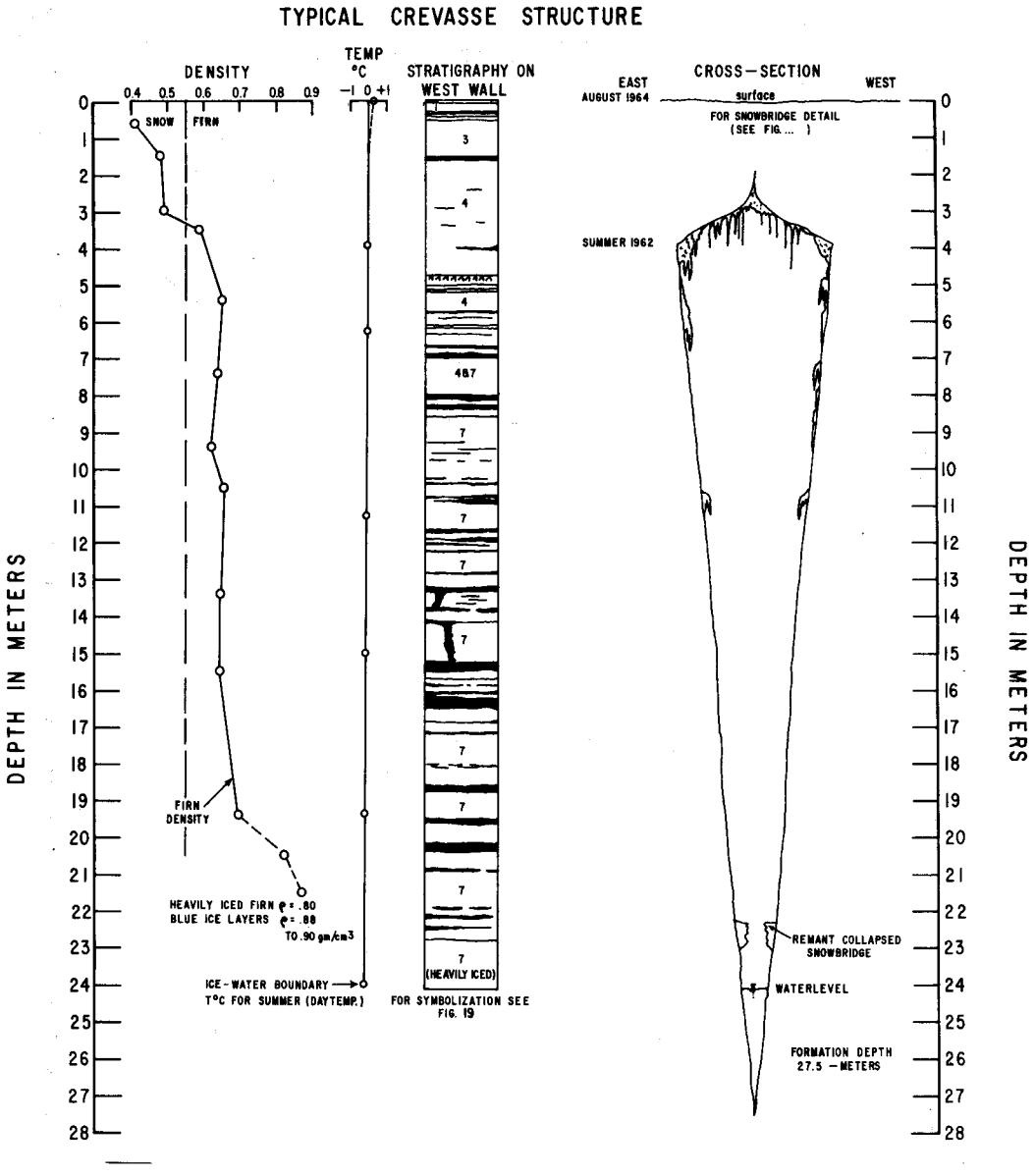

Figure 19. Stratigraphic, geophysical and morphological features of a typical crevasse.

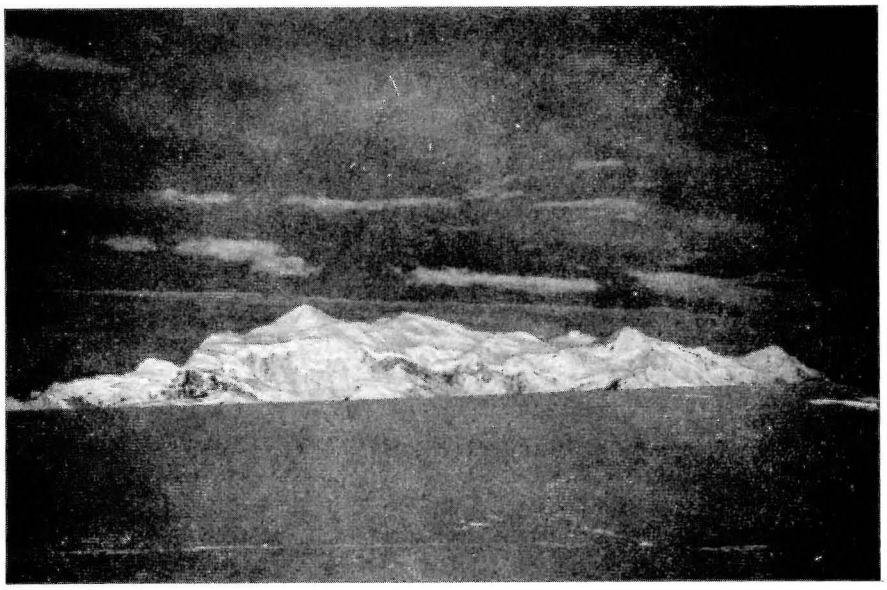

Plate 1. View S.W. from Divide Camp showing barrier of Mt. Logan Massif. Foreground topography is typical of the divide and upper North Arm of the Kaskawulsh Glacier.

Plate 2. View N.E. from Crevasse Camp looking down the North Arm of the Kaskawulsh Glacier.

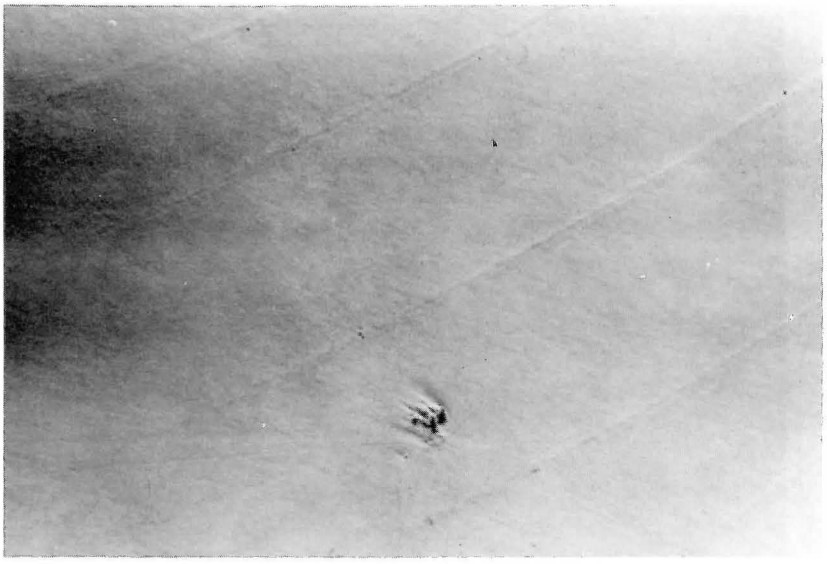

Plate 3. Aerial view of Crevasse Camp and transverse crevasse field. Line of pits is perpendicular to the crevasse traces which are convex up glacier.

Plate 4. Aerial oblique view of the crevasse field. Crevasse Camp is just visible.

Plate 5. Aerial oblique view showing the geometry of the transverse crevasses. To the south a small ice-fall and marginal crevasses complicate the pattern.

Plate 6. View looking upward through the snow-bridge, from 20 meters below the surface.

Plate 7. Icicles on base of snow-bridge.

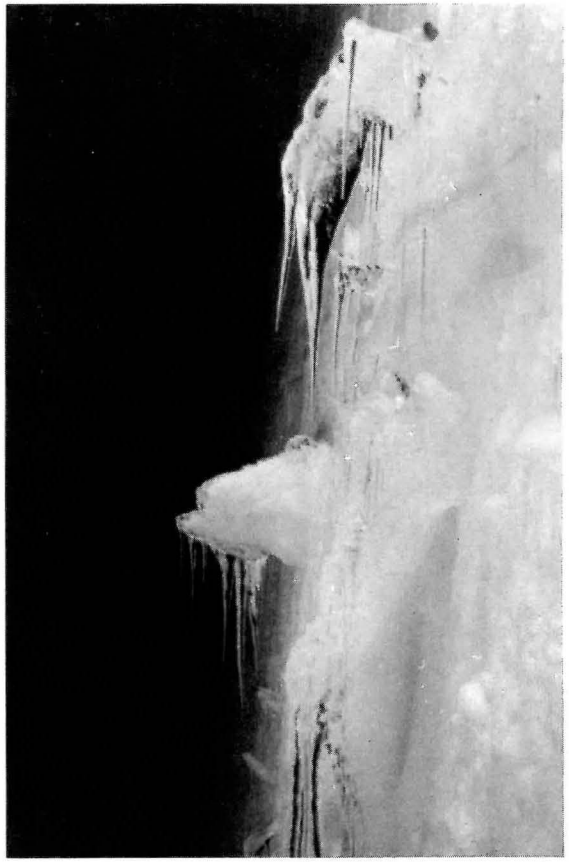

Plate 8. Crevasse wall growths and icicles.